

3

Pollutant Formation and Control in Combustion

In this chapter we study the formation of pollutants in combustion systems. Our ultimate objectives are to be able to predict the levels of pollutants in the combustion products, leaving practical combustion systems, and to use such predictions to suggest combustion modifications to achieve lower emission levels. We focus on the basic mechanisms of pollutant formation in continuous-flow combustors. Internal combustion engines and gas-cleaning systems will be treated in subsequent chapters.

3.1 NITROGEN OXIDES

Nitrogen oxides are important air pollutants, the primary anthropogenic source of which is combustion. Motor vehicles account for a large fraction of the nitrogen oxide emissions, but stationary combustion sources ranging from electric power generating stations to gas-fired cooking stoves also release nitrogen oxides.

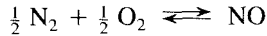
Both nitric oxide, NO, and nitrogen dioxide, NO₂, are produced in combustion, but the vast majority of nitrogen oxides are emitted as NO (recall Table 1.4). Because NO is converted to NO₂ in the atmosphere, emissions of both species frequently are lumped together with the designation NO_x. When NO_x emissions are presented in mass units, the mass of NO_x is calculated as if all the NO had been converted to NO₂. Because NO is the predominant NO_x species formed in combustion, we shall concentrate on it in this section.

Nitric oxide is formed both from atmospheric nitrogen, N₂, and from nitrogen contained in some fuels. The latter source depends on the fuel composition and is not important for fuels with low nitrogen contents but is a major source of NO_x in coal

combustion. Nitric oxide can be formed, however, when any fuel is burned in air because of the high-temperature oxidation of N_2 . We begin our discussion with the fixation of atmospheric nitrogen.

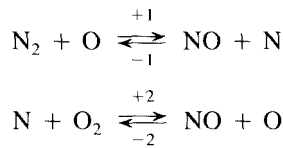
3.1.1 Thermal Fixation of Atmospheric Nitrogen

The formation of NO by oxidation of atmospheric nitrogen can be expressed in terms of the overall reaction

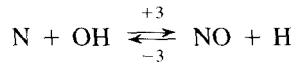


which is highly endothermic [i.e., $\Delta h_p^\circ(298\text{ K}) = 90.4\text{ kJ mol}^{-1}$]. As a result, the equilibrium concentration of NO is high at the very high temperatures encountered near stoichiometric combustion and decreases rapidly away from that point.

Even though we express the overall reaction as above, the direct reaction of N_2 with O_2 is too slow to account for significant NO formation. Free oxygen atoms, produced in flames by dissociation of O_2 or by radical attack on O_2 , attack nitrogen molecules and begin a simple chain mechanism that was first postulated by Zeldovich et al. (1947), that is,



The concentration of O_2 is low in fuel-rich combustion, so reaction 2 is less important than in fuel-lean combustion. Reaction with the hydroxyl radical eventually becomes the major sink for N:



The rate constants for the so-called extended Zeldovich mechanism are (Hanson and Salimian, 1984)

$$\begin{aligned} k_{+1} &= 1.8 \times 10^8 e^{-38,370/T} \text{ m}^3 \text{ mol}^{-1} \text{ s}^{-1} \\ k_{-1} &= 3.8 \times 10^7 e^{-425/T} \text{ m}^3 \text{ mol}^{-1} \text{ s}^{-1} \\ k_{+2} &= 1.8 \times 10^4 T e^{-4680/T} \text{ m}^3 \text{ mol}^{-1} \text{ s}^{-1} \\ k_{-2} &= 3.8 \times 10^3 T e^{-20,820/T} \text{ m}^3 \text{ mol}^{-1} \text{ s}^{-1} \\ k_{+3} &= 7.1 \times 10^7 e^{-450/T} \text{ m}^3 \text{ mol}^{-1} \text{ s}^{-1} \\ k_{-3} &= 1.7 \times 10^8 e^{-24,560/T} \text{ m}^3 \text{ mol}^{-1} \text{ s}^{-1} \end{aligned}$$

The high activation energy of reaction 1, resulting from its essential function of breaking the strong N_2 triple bond, makes this the rate-limiting step of the Zeldovich mechanism.

Due to the high activation energy, NO production by this mechanism proceeds at a slower rate than the oxidation of the fuel constituents and is extremely temperature sensitive. The production of atomic oxygen required for the first reaction is also highly temperature sensitive.

To understand the rate of NO formation, let us examine the rate equations corresponding to the mechanism of reactions 1-3. For example, the net rates of formation of NO and N are

$$R_{NO} = k_{+1}[N_2][O] - k_{-1}[N][NO] + k_{+2}[N][O_2] - k_{-2}[NO][O] + k_{+3}[N][OH] - k_{-3}[NO][H] \quad (3.1)$$

$$R_N = k_{+1}[N_2][O] - k_{-1}[N][NO] - k_{+2}[N][O_2] + k_{-2}[NO][O] - k_{+3}[N][OH] + k_{-3}[NO][H] \quad (3.2)$$

The concentrations of O, H, and OH are required for calculation of the N and NO formation rates. The high activation energy of the initial N₂ attack allows us to make an important simplification. Since the reaction rate is fast only at the highest temperatures, most of the reaction takes place after the combustion reactions are complete and before significant heat is transferred from the flame. It is a reasonable first approximation, therefore, to assume that the O, H, and OH radicals are present in their equilibrium concentrations.

This suggests a simplification proposed by Lavoie et al. (1970). At thermodynamic equilibrium, we may write

$$k_{+1}[N_2]_e[O]_e = k_{-1}[N]_e[NO]_e \quad (3.3)$$

We may define the equilibrium, one-way rate of reaction as

$$R_1 = k_{+1}[N_2]_e[O]_e = k_{-1}[N]_e[NO]_e \quad (3.4)$$

Similarly, at equilibrium

$$R_2 = k_{+2}[N]_e[O_2]_e = k_{-2}[NO]_e[O]_e \quad (3.5)$$

$$R_3 = k_{+3}[N]_e[OH]_e = k_{-3}[NO]_e[H]_e \quad (3.6)$$

Further defining the quantities,

$$\alpha = \frac{[NO]}{[NO]_e}$$

$$\beta = \frac{[N]}{[N]_e}$$

the rate equations may now be expressed in the abbreviated form

$$R_{NO} = R_1 - R_1\alpha\beta + R_2\beta - R_2\alpha + R_3\beta - R_3\alpha \quad (3.7)$$

$$R_N = R_1 - R_1\alpha\beta - R_2\beta + R_2\alpha - R_3\beta + R_3\alpha \quad (3.8)$$

We must determine the N atom concentration if we are to calculate the rate of NO formation. Since the activation energy for oxidation of the nitrogen atom is small and, for fuel-lean conditions, the reaction involves O_2 , a major component of the gas, the free nitrogen atoms are consumed as rapidly as they are generated, establishing a quasi-steady state. Setting the left-hand side of (3.8) equal to zero and solving for the steady-state nitrogen atom concentration, we find

$$\beta_{ss} = \frac{R_1 + R_2\alpha + R_3\alpha}{R_1\alpha + R_2 + R_3} = \frac{\kappa + \alpha}{\kappa\alpha + 1} \quad (3.9)$$

where

$$\kappa = \frac{R_1}{R_2 + R_3} \quad (3.10)$$

Substituting (3.9) into (3.7) yields a rate equation for NO formation in terms of α and known quantities,

$$R_{NO} = \frac{2R_1(1 - \alpha^2)}{1 + \kappa\alpha} \quad (3.11)$$

In general, the NO formation rate is expressed based on the total mass in the system [see (A.7)–(A.10)]

$$R_{NO} = \rho \frac{d}{dt} \left(\frac{[NO]}{\rho} \right)$$

For constant temperature and pressure, this may be written as a differential equation for α :

$$\frac{d\alpha}{dt} = \frac{1}{[NO]_e} \frac{2R_1(1 - \alpha^2)}{1 + \kappa\alpha} \quad (3.12)$$

The initial NO formation rate (at $\alpha = 0$) is twice the rate of reaction 1. Figure 3.1 shows how this initial rate varies with equivalence ratio for adiabatic combustion. The conditions for these calculations are the same as for the equilibrium calculations previously shown in Figures 2.6 and 2.7. The sharp peak near stoichiometric is due to the high flame temperatures.

Equation (3.12) can be integrated analytically to describe NO formation in a constant-temperature system. Assuming that there is no NO present initially (i.e., $\alpha = 0$ at $t = 0$), the result is

$$(1 - \kappa) \ln(1 + \alpha) - (1 + \kappa) \ln(1 - \alpha) = \frac{t}{\tau_{NO}} \quad (3.13)$$

where the characteristic time for NO formation is

$$\tau_{NO} = \frac{[NO]_e}{4R_1} \quad (3.14)$$

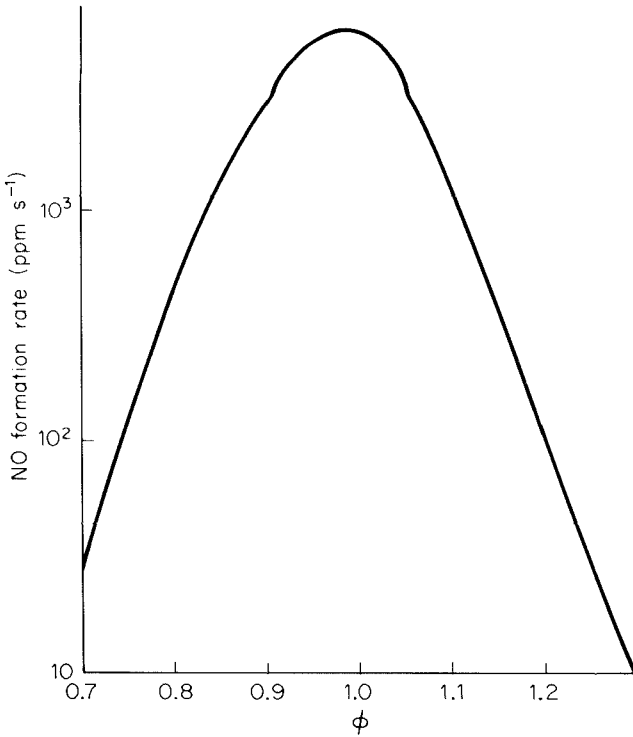


Figure 3.1 Variation of the initial NO formation rate with equivalence ratio for adiabatic combustion of kerosene with composition $CH_{1.8}$.

This approach to equilibrium is illustrated in Figure 3.2. It is apparent that τ_{NO} corresponds to the time that would be required for NO to reach the equilibrium level if the reaction continued at its initial rate and were not slowed by the reverse reactions.

Two major assumptions have been made in the derivation of (3.11): (1) a quasi-steady state for the nitrogen atom concentration and (2) equilibrium concentrations for the O, H, and OH radicals. The validity of the first assumption can readily be examined.

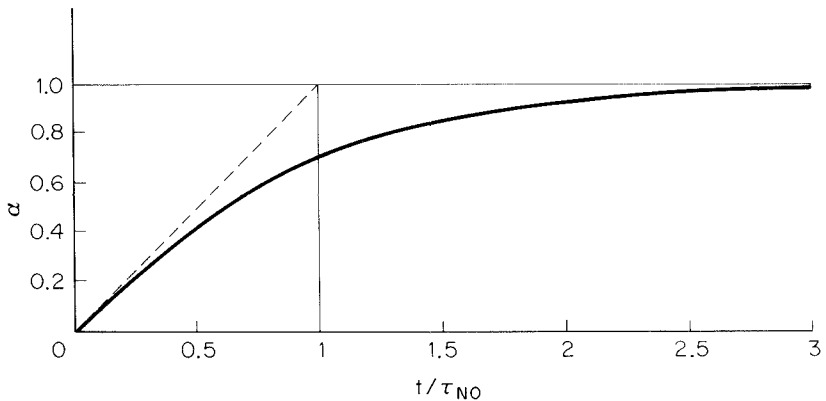


Figure 3.2 Approach of the dimensionless NO concentration to equilibrium.

If we consider the time required to achieve this steady state initially, which is when the NO concentration is small, and only the forward reactions need be considered. The rate equation for the nitrogen atom concentration becomes

$$[N]_e \frac{d\beta}{dt} = R_1 - (R_2 + R_3)\beta \quad (3.15)$$

with the initial condition of $\beta = 0$ at $t = 0$. Integrating yields

$$\beta = \kappa \left[1 - \exp\left(-\frac{t}{\tau_N}\right) \right] \quad (3.16)$$

where

$$\tau_N = \frac{[N]_e}{R_2 + R_3} \quad (3.17)$$

For the quasi-steady N assumption to be valid, τ_N must be much smaller than τ_{NO} . Comparison of the two time scales for adiabatic combustion indicates that τ_N is several orders of magnitude smaller than τ_{NO} throughout the range of equivalence ratios where NO formation by the Zeldovich mechanism is significant. Only for extremely fuel-rich combustion does τ_N approach τ_{NO} , but in this regime other reactions must be included.

Example 3.1 Thermal-NO_x Formation

In a gas turbine, air is compressed adiabatically from atmospheric pressure and 290 K to a pressure of 10 atm. Fuel (aviation kerosene, CH_{1.88}, LHV = 600 kJ (mol C)⁻¹) is injected into the hot air, mixed rapidly, and burned. After a brief residence in the primary combustion zone, typically 0.005 s, the combustion products are diluted with additional compressed air to lower the temperature below the limiting turbine inlet temperature. Assuming perfect mixing and adiabatic combustion at $\phi = 0.8$ in the primary zone, estimate the mole fraction of NO_x formed in the primary combustion zone.

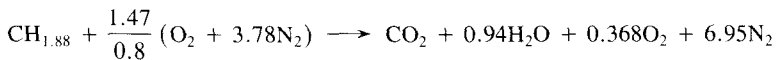
To calculate the NO formation rate, we first need to know the flame temperature. That, in turn, requires knowledge of the temperature of the air following compression. For adiabatic and reversible compression of an ideal gas from pressure p_1 and p_2 , the temperature rises according to

$$T_2 p_2^{-(\gamma-1)/\gamma} = T_1 p_1^{-(\gamma-1)/\gamma}$$

where $\gamma = c_p/c_v$ is the ratio of specific heats. For air, $\gamma = 1.4$, so

$$T_2 = T_1 \left(\frac{p_1}{p_2} \right)^{-(\gamma-1)/\gamma} = 290 \left(\frac{1}{10} \right)^{-(0.4/1.4)} = 560 \text{ K}$$

Assuming complete combustion, the combustion stoichiometry becomes



The energy equation may be written as

$$\begin{aligned}
 & [h(T) - h(T_0)]_{\text{CO}_2} + 0.94[h(T) - h(T_0)]_{\text{H}_2\text{O}} + 0.368[h(T) - h(T_0)]_{\text{O}_2} \\
 & + 6.95[h(T) - h(T_0)]_{\text{N}_2} - 1.84[h(T_a) - h(T_0)]_{\text{O}_2} - 6.95[h(T_a) - h(T_0)]_{\text{N}_2} \\
 & - [h(T_f) - h(T_0)]_{\text{CH}_{1.88}} + \Delta h_{\text{cl}}(T_0) = 0
 \end{aligned}$$

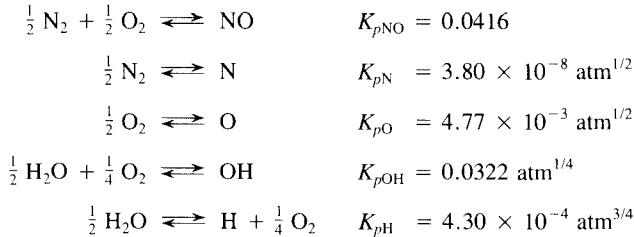
Using the data from Table 2.5, the sensible enthalpy terms become

$$[h(T) - h(T_0)]_i = a_i(T - T_0) + \frac{b_i}{2}(T_i^2 - T_0^2)$$

Neglecting the small sensible enthalpy term for the fuel, we find

$$T = 2304 \text{ K}$$

To calculate the NO formation rate, we need the equilibrium concentrations of NO, N, O, OH, and H. Use the following reactions and equilibrium constants:



From the combustion stoichiometry and these equilibrium relationships, we calculate

$$\begin{aligned}
 y_{\text{N}_2} &= 0.751 & y_{\text{N}_e} &= 1.04 \times 10^{-8} \\
 y_{\text{O}_2} &= 0.0397 & y_{\text{O}_e} &= 3.01 \times 10^{-4} \\
 y_{\text{H}_2\text{O}} &= 0.102 & y_{\text{OH}_e} &= 2.58 \times 10^{-3} \\
 y_{\text{NO}_e} &= 7.18 \times 10^{-3} & y_{\text{H}_e} &= 5.47 \times 10^{-5}
 \end{aligned}$$

The equilibrium, one-way reaction rates are

$$\begin{aligned}
 R_1 &= k_{+1}c^2y_{\text{N}_2}y_{\text{O}_e} = 6.61 \text{ mol m}^{-3} \text{ s}^{-1} \\
 R_2 &= k_{+2}c^2y_{\text{N}_e}y_{\text{O}_2} = 6.29 \text{ mol m}^{-3} \text{ s}^{-1} \\
 R_3 &= k_{+3}c^2y_{\text{N}_e}y_{\text{OH}_e} = 4.39 \text{ mol m}^{-3} \text{ s}^{-1}
 \end{aligned}$$

leading to a characteristic time for NO formation of

$$\begin{aligned}
 \tau_{\text{NO}} &= \frac{[\text{NO}]_e}{4R_1} = \frac{7.18 \times 10^{-3} \times 52.9 \text{ mol m}^{-3}}{4 \times 6.61 \text{ mol m}^{-3} \text{ s}^{-1}} \\
 &= 0.0143 \text{ s}
 \end{aligned}$$

which is more than the residence time of 0.005 s, so we do not expect NO to reach equilibrium. To find the actual conversion, we can solve (3.13) by iteration using, from (3.10),

$\kappa = 0.619$. The result is

$$\alpha = \frac{y_{\text{NO}}}{y_{\text{NO}_e}} = 0.165$$

or

$$\begin{aligned} y_{\text{NO}} &= \alpha y_{\text{NO}_e} = 1.18 \times 10^{-3} \\ &= 1180 \text{ ppm} \end{aligned}$$

It is also worthwhile to examine the validity of the assumptions regarding the nitrogen atoms. The steady-state nitrogen atom level is given by (3.9)

$$\beta_{ss} = \frac{\kappa + \alpha}{1 + \kappa\alpha} = 0.711$$

The time required to reach steady state is estimated by (3.17):

$$\tau_N = \frac{[\text{N}]_e}{R_2 + R_3} = \frac{c y_{\text{N}_e}}{R_1/\kappa} = 5.15 \times 10^{-8} \text{ s}$$

Clearly, the steady state is achieved on a time scale that is very short compared to that for NO formation.

3.1.2 Prompt NO

Nitric oxide can be formed from N_2 in the air through a mechanism distinct from the thermal mechanism. This other route, leading to what is termed *prompt* NO, occurs at low temperature, fuel-rich conditions and short residence times. This mechanism was first identified by C.P. Fenimore in 1971. In studying NO formation in fuel-rich hydrocarbon flames, Fenimore found that NO concentration profiles in the postflame gases did not extrapolate to zero at the burner surface. He did not find such behavior in either CO or H_2 flames, which are not hydrocarbons. Fenimore concluded that the NO formed early in the flame was the result of the attack of a hydrocarbon free radical on N_2 , in particular by



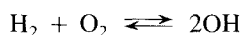
The rate of oxidation of the fuel is usually sufficiently rapid that fuel radicals such as CH are at such low concentrations that reactions such as $\text{CH} + \text{N}_2$ are negligible. Under certain fuel-rich conditions, however, such hydrocarbon radicals can reach high enough concentration levels that reactions with N_2 can become an important mode of breaking the N_2 bond and, in turn, be responsible for significant NO formation. Such reactions appear to have relatively low activation energy and can proceed at a rate comparable to that of the oxidation of the fuel. Because of the early (that is, within the flame rather than in the post-flame gases) formation of NO by this mechanism, relative to that formed by the Zeldovich mechanism, NO thus formed is often referred to as *prompt* NO (Bowman, 1975). Even in fuel-lean flames where the hydrocarbon radical attack of N_2 is unimportant, the nonequilibrium chemistry in the flame front can lead to prompt NO

formation. The quantity of NO formed in the flame zone increases as the equivalence ratio increases. Miller and Fisk (1987) have found that in the combustion of methane in a well-stirred reactor at 2 ms residence time the $\text{CH} + \text{N}_2$ reaction accounts for virtually all of the fixed nitrogen at equivalence ratios greater than 1.2; in fact, the mechanism explains 25 percent of the fixed nitrogen even at stoichiometric conditions. Longer residence times, however, increasingly favor the Zeldovich mechanism. The prompt NO route adds the complication that fixed nitrogen can be emitted from combustors in forms other than NO_x , that is HCN or products of its oxidation.

Prediction of NO formation within the flame requires coupling the NO kinetics to an actual hydrocarbon combustion mechanism. As noted in Chapter 2, hydrocarbon combustion involves several steps, that is, attack of the hydrocarbon molecules leading to CO formation, CO oxidation, and radical consumption by three-body recombination reactions. Since the attack of N_2 by O is highly endothermic, most prompt NO is formed relatively late in fuel-lean flames, after CO has been formed but before the final C/H/O equilibrium is achieved. Sarofim and Pohl (1973) proposed estimating the concentrations of the radicals in the region of the flame where CO is consumed using a partial equilibrium approximation. In such an approximation, the rapid bimolecular reactions of the radicals (reactions 10–15 of the hydrocarbon oxidation mechanism presented in Section 2.4.1) are assumed to be locally equilibrated long before the CO oxidation,



and the three-body recombination reactions approach equilibrium. After some rearrangement, the radical exchange reactions yield overall reactions that relate the radical concentrations to those of the major species:



Sarofim and Pohl (1973) used such relationships to calculate the concentrations of H, O, and OH based on measurements of the major species concentrations in a laminar flame front. The partial equilibrium radical concentrations were then used to make improved estimates of the rate of NO formation within the flame front by the reactions of the Zeldovich mechanism. The calculated NO levels in the flame were in reasonable agreement with experimental observations for fuel-lean and slightly fuel-rich flames.

To predict NO formation in the flame front, the kinetics of the CO oxidation and the three-body recombination reactions must be followed along with the kinetics of NO formation. Using the partial-equilibrium approximation, overall rate expressions can be derived for these additional processes, as will be demonstrated in our discussion of CO oxidation. The intricate coupling of the NO chemistry to the hydrocarbon oxidation mechanism in fuel-rich flames precludes the development of simplified models for such flames.

Although NO formation rates in the vicinity of the flame can be large, the quantity of NO formed in the postflame region is large compared to the prompt NO in many

practical combustions. The coupling between NO formation and the combustion process, to a first approximation, can be neglected in this case, and the extended Zeldovich mechanism and equilibrium properties of the postcombustion gases can be used to calculate NO emissions. As NO_x emission levels are reduced to very low levels, however, the relative importance of the prompt NO can be expected to increase, possibly limiting the effectiveness of the NO_x emission controls.

3.1.3 Thermal- NO_x Formation and Control in Combustors

The inhomogeneities in composition in nonpremixed combustion strongly influence NO_x emissions. The experiments and approach of Pompei and Heywood (1972) provide a convenient vehicle for exploring the role of turbulent mixing in NO_x formation. In Section 2.5.4 we discussed their use of oxygen and a Gaussian composition distribution in the estimation of the degree of inhomogeneity in a nonpremixed combustor. The influence of inhomogeneity on the initial rate of NO formation can be seen by calculating the mean NO formation rate. In the discussion to follow, we limit our attention to NO formation by the Zeldovich mechanism before the NO concentration has accumulated to the point that the reverse reactions become significant. Prompt NO will not be considered.

The mean NO formation rate

$$\overline{R_{\text{NO}}} = \overline{\rho} \int_0^{\infty} \frac{R_{\text{NO}}(\phi)}{\rho(\phi)} p(\phi) d\phi \quad (3.18)$$

is shown in Figure 3.3 as a function of equivalence ratio for several values of the segregation parameter, $S = \sigma/\overline{\phi}$. For $S = 0$ (perfect mixing) we see the sharp peak in the NO formation rate. Poorer mixing substantially reduces the maximum NO formation rate but extends the domain of significant NO formation to lower equivalence ratios.

The strong dependence of the Zeldovich kinetics on temperature provides the major tool used in the control of NO formation in combustion systems. Any modifications of the combustion process that reduce the peak temperatures in the flame can be used to reduce NO_x emissions. Because of this temperature dependence, the NO formation rate varies strongly with equivalence ratio, with a sharp peak near $\phi = 1$, as was shown in Figure 3.1. Reduction of the equivalence ratio is one possible method for NO_x control, but as we have just seen, this method is substantially less effective in nonpremixed combustion than simple theory might predict. While chemical considerations would suggest that reducing $\overline{\phi}$ from 0.9 to 0.7 should reduce the NO_x formation rate by two orders of magnitude, a typical combustor with $S \approx 0.5$ would show virtually no change. Fuel-lean combustion reduces the flame temperature by diluting the combustion gases with excess air. If a material that does not participate in the combustion reactions is used as a diluent instead of air, the adiabatic temperature of stoichiometric combustion can be reduced and more effective control can be achieved. One common method is flue gas recirculation (FGR), in which the most readily available nonreactive gas, cooled com-

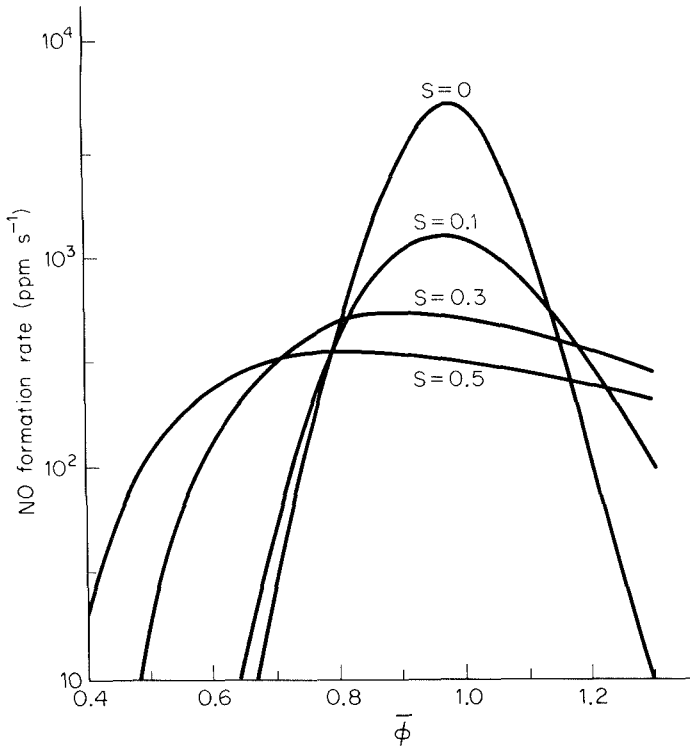


Figure 3.3 Influence of mixing on the NO formation rate in adiabatic combustion of kerosene, $CH_{1.8}$.

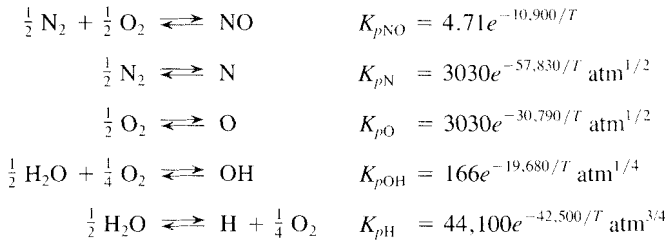
bustion products, is mixed with the combustion air. This approach is used extensively in utility boilers and other large stationary combustors. Injection of other diluents such as water or steam can also be used to reduce the NO formation rates, but the penalty in reduced system efficiency may be larger.

Modifications of the combustion system design or operation are also used to control NO_x emissions. One way the combustion rate is lowered is to introduce only a fraction of the air with fuel, with the remaining air being added in so-called overfire air ports above the main burners. Heat transfer from the fuel-rich region lowers the ultimate flame temperature and, therefore, the NO formation rate when the air required to complete the combination is finally added. Different types of burners yield widely different NO_x emission levels depending on the time required for combustion and the amount of heat rejected during the combustion process. A long flame that slowly entrains air allows a large fraction of the heat of combustion to be transferred to the furnace walls before combustion is complete, while a highly turbulent flame with intense recirculation may be more nearly adiabatic. NO_x emissions from the former type of burner are generally lower than those from the latter.

Example 3.2 Thermal-NO_x Control

To control thermal-NO_x formation, it is necessary to reduce the temperature to slow the rate of N₂ oxidation. One approach is to inject liquid water into the fuel-air mixture to reduce the flame temperature. Determine how much liquid water would be required to lower NO_x production for the conditions of Example 3.1 by 90%.

It is useful first to estimate how much the temperature must be reduced to achieve the necessary reduction in the NO formation rate. Since the final NO level was well below equilibrium, a 90% reduction in emissions corresponds approximately to a 90% reduction in R_1 . We need to determine y_{O_e} . Applying van't Hoff's relation, we find the equilibrium constants:



R_1 becomes

$$\begin{aligned} R_1 &= k_1 c^2 y_{\text{N}_2} y_{\text{O}_e} = k_1 c^2 y_{\text{N}_2} K_{p\text{O}}^{-1/2} y_{\text{O}_2}^{1/2} \\ &= 1.8 \times 10^8 e^{-38,370/T} \left(\frac{1.013 \times 10^6}{8.314T} \right)^2 \times 0.751 \\ &\quad \times 3030e^{-30,790/T} 10^{-1/2} \times 0.0397^{1/2} \\ &= 3.83 \times 10^{20} T^{-2} e^{-69,160/T} \text{ mol m}^{-3} \text{ s}^{-1} \end{aligned}$$

For 90% reduction in NO_x formation, we want $R_1 \approx 0.661 \text{ mol m}^{-3} \text{ s}^{-1}$. Solving iteratively for temperature, we find

$$T \approx 2130 \text{ K}$$

Thus it appears that T must be reduced by only 175 K to achieve 90% control.

The amount of water required for this reduction is determined by a first-law analysis. The energy equation becomes

$$\begin{aligned} &[h(T) - h(T_0)]_{\text{CO}_2} + (0.94 + \zeta) [h(T) - h(T_0)]_{\text{H}_2\text{O}} + 0.368 [h(T) - h(T_0)]_{\text{O}_2} \\ &+ 6.95 [h(T) - h(T_0)]_{\text{N}_2} - 1.84 [h(T_a) - h(T_0)]_{\text{O}_2} \\ &- 6.95 [h(T_a) - h(T_f)]_{\text{N}_2} - [h(T_f) - h(T_0)]_{\text{CH}_{1.88}} \\ &- \zeta [h(T_w) - h(T_0)] + \zeta \Delta h_v(T_0) + \Delta h_{cL}(T_0) \end{aligned}$$

where ζ is the number of moles of water added per mole of carbon and Δh_v is the molar latent heat of vaporization of the water.

Using data from Table 2.5, we find

$$\begin{aligned} (289 + 32.5\zeta) (T - T_0) + (0.0190 + 0.00431\zeta) (T^2 - T_0^2) \\ - 259.4(T_a - T_0) - 0.0139(T_a^2 - T_0^2) + 44,000\zeta - 600,000 = 0 \end{aligned}$$

Recalling from Example 3.1 that $T_a = 560$ K, and imposing $T = 2130$ K, this becomes

$$122,711\zeta - 57,126 = 0$$

or

$$\zeta = 0.47$$

Thus we require 0.60 kg of water to be added for every 1 kg of fuel burned.

Now let us confirm the amount of NO formed. The combustion product composition for $T = 2130$ K and $\zeta = 0.47$ is

$$\begin{aligned} y_{N_2} &= \frac{6.95}{9.26 + 0.47} = 0.714 & y_{N_e} &= 1.31 \times 10^{-9} \\ y_{O_2} &= 0.0378 & y_{O_e} &= 9.82 \times 10^{-5} \\ y_{H_2O} &= 0.145 & y_{OH_e} &= 1.52 \times 10^{-3} \\ y_{CO_2} &= 0.103 & y_{H_e} &= 4.63 \times 10^{-4} \\ y_{NO_e} &= 4.64 \times 10^{-3} \end{aligned}$$

from which we find

$$R_1 = 0.620 \text{ mol m}^{-3} \text{ s}^{-1}$$

$$R_2 = 0.690$$

$$R_3 = 0.369$$

and

$$\tau_{NO} = \frac{c y_{NO_e}}{4R_1} = 0.107 \text{ s}$$

$$\kappa = \frac{R_1}{R_2 + R_3} = 0.585$$

For a residence time of 0.005 s, we find by iteration

$$\alpha = 2.33 \times 10^{-2}$$

and

$$y_{NO} = 1.08 \times 10^{-4} = 108 \text{ ppm}$$

Thus, emissions would be reduced by 91% through the addition of 0.60 kg of water for each 1 kg of fuel burned. The effects of this large water addition on engine performance would also have to be considered in assessing this approach to NO_x emission control.

3.1.4 Fuel- NO_x

Many fuels contain organically bound nitrogen that is readily oxidized to NO during combustion (Sarofim and Flagan, 1976). Crude oils contain 0.1 to 0.2% nitrogen on a mass basis, but levels as high as 0.5% are found in some oils. In refining the oil, this

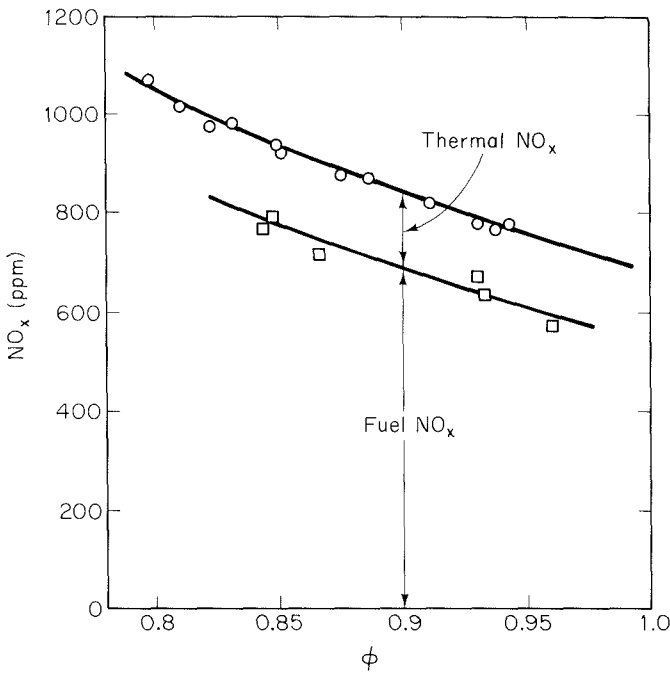


Figure 3.4 Contributions of thermal- NO_x and fuel- NO_x to total NO_x emissions in the laboratory pulverized coal combustion experiments of Pershing and Wendt (1977). Reprinted by permission of The Combustion Institute.

nitrogen is concentrated in the residual fractions, that is, in that portion of the oil that is most likely to be burned in large combustion systems such as power plants or industrial boilers rather than used as transportation fuels. Coal typically contains 1.2 to 1.6% nitrogen. The range of nitrogen contents of coals is much narrower than that of the sulfur contents. Thus burning a low-nitrogen coal is not a practical solution to the problems of fuel- NO_x emissions from coal-fired boilers unless one dilutes the coal with a low-nitrogen fuel oil. New fuel sources may further aggravate the problems associated with fuel-nitrogen. Some of the major shale oil deposits in the United States contain 2 to 4% nitrogen.

The contribution of fuel-nitrogen to NO_x emissions is most clearly shown by experiments in which the possibility of forming NO from N_2 is eliminated. Pershing and Wendt (1977) compared the NO_x emissions from combustion of pulverized coal in air to the emissions when the air was replaced with a mixture of oxygen, argon, and carbon dioxide that was selected to achieve the same adiabatic flame temperature as combustion at the same equivalence ratio in air. The former case includes both NO formed from N_2 and NO from the fuel nitrogen while fuel-nitrogen contributes to NO formation in the latter case. The data of Pershing and Wendt, shown in Figure 3.4, clearly demonstrate

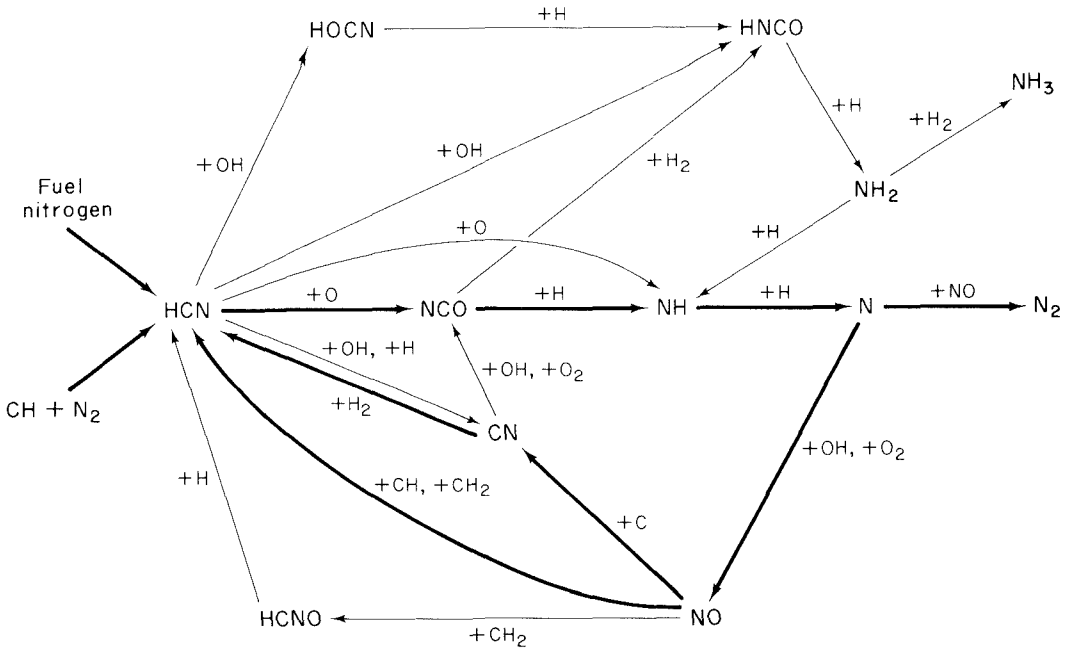


Figure 3.5 Reaction paths in rich hydrocarbon flames ($1.0 < \phi < 1.5$). Thick arrows show the dominant steps. (Miller and Fisk, 1987).

the importance of the fuel-nitrogen. Even though fuel-nitrogen was the major source of NO_x , not all of the fuel-nitrogen was converted to NO. In these experiments, 20 to 30% conversion was observed.

The nitrogen in these fuels is present predominantly in pyridine and pyrrole groups:



pyridine



pyrrole

In the early phases of combustion, these molecules undergo ring schism. Further attack yields molecules such as HCN or NH₃ or nitrogen-containing radicals such as NH₂ or CN. These reactions are an integral part of the combustion of the parent hydrocarbon and therefore proceed rapidly in the combustion process.

The principal paths by which fuel nitrogen species are combusted are thought to begin with the conversion of the fuel nitrogen molecule to hydrogen cyanide, HCN (Haynes et al., 1975). We recall that the key step in prompt NO formation is also HCN

formation by $\text{CH} + \text{N}_2$. Figure 3.5 depicts the current understanding of the reaction paths by which hydrogen cyanide is converted to NO and other products in rich hydrocarbon flames ($1.0 < \phi < 1.5$) (Miller and Fisk, 1987). The thick arrows show the dominant steps. Under most conditions the dominant path from HCN to NO is the sequence initiated by reaction of HCN with atomic oxygen,



followed by



and



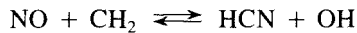
with the nitrogen atom leading to NO,



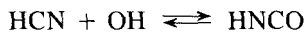
The NO produced in this way may itself react with N atoms to form N_2 ,



or it can be recycled to form CN or HCN by reaction with hydrocarbon free radicals,



The reaction paths through CN and HNCO can also be important, for example the sequence,

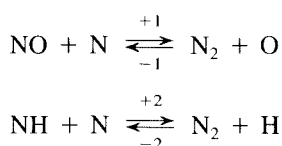


leads to ammonia formation.

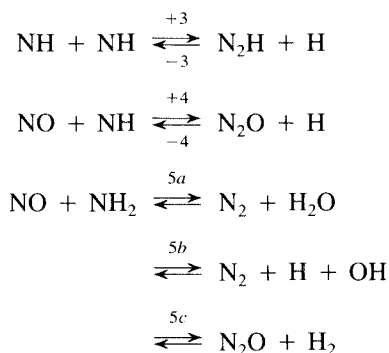
Under leaner conditions the oxygen atom concentration may be sufficiently high that NCO and CN may react with oxygen atoms to produce NO directly or indirectly. NH may react with O or OH to produce NO directly or indirectly through HNO, for example



The nitrogen species produced by this chain of reactions can also react to form N_2 . The formation of N_2 from fuel-nitrogen requires the reaction of two fixed nitrogen species, for example,

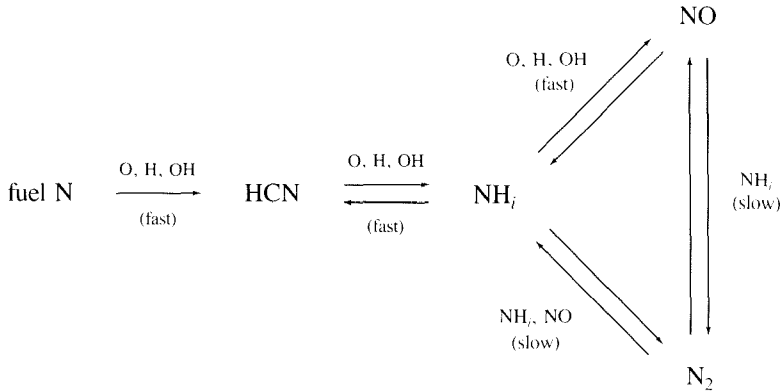


Note that the reverse of reaction 1 is the first reaction of the Zeldovich mechanism, which, as we have already seen, is the predominant reaction contributing to NO formation from N_2 in fuel-lean or near stoichiometric combustion. Other reactions that form the strong nitrogen–nitrogen bond may ultimately lead to N_2 formation. Such reactions include



The $\text{NO} + \text{NH}_2$ reaction has three possible outcomes but may be described approximately by a single rate expression for the net formation of the nitrogen–nitrogen bond (Hanson and Salimian, 1984). The concentrations of the fixed nitrogen species are relatively low, so these reactions that are second order in fixed nitrogen (RN) proceed slowly.

The fuel-nitrogen chemistry may be described schematically by



Since the reactions leading to NH_i and NO are much faster than those leading to N_2 formation, a rate-constrained partial-equilibrium model can be developed to describe the rate at which fuel-nitrogen is converted to N_2 (Flagan et al., 1974).

We begin our quantitative discussion of fuel-nitrogen chemistry by examining how the fuel-nitrogen would be distributed if, during the initial hydrocarbon attack, no N_2 formation were to occur. Because the formation of N_2 requires the reaction of two fixed nitrogen species, one being present only in very small concentrations due to the rapid consumption of N , NH and NH_2 , N_2 formation proceeds much more slowly than the flame chemistry. Hence the distribution of the fuel-nitrogen subject to the constraint that no N_2 be formed from fuel-N is a reasonable approximation of the gas composition immediately downstream of the flame. This partial-equilibrium distribution of single nitrogen species for adiabatic combustion of a fuel oil containing 1% by weight of nitrogen is illustrated in Figure 3.6. The total amount of fuel-nitrogen in the parent fuel is indicated by the dashed line labeled RN . Given the constraint on equilibrium, the sum of the concentrations of all single nitrogen (RN) species must equal this value. At equivalence ratios from 0.1 to 1.6, the major fixed nitrogen species in this partial equilibrium is NO . At higher equivalence ratios, NH_3 dominates. N_2 is the primary species in very fuel-lean gases. Nitrogen atoms and other radicals are present only in very low concentrations.

The NO concentration at full thermodynamic equilibrium (NO_e) is also shown by a dashed line. The NO derived from the fuel-nitrogen is below the equilibrium level for equivalence ratios ranging from 0.5 to 1.05, so additional NO formation from N_2 may be expected in this regime. The primary reactions leading to the fixation of N_2 are those of the Zeldovich mechanism, so the model developed in Section 3.1.1 describes the N_2 fixation in this regime. Outside this region, the conversion of fixed nitrogen to N_2 is favored thermodynamically. The rate at which N_2 is formed from fuel-nitrogen intermediates in these rich and lean regimes can be examined with the partial-equilibrium approach. The basic assumption of this model is that within the flame, the fuel-nitrogen is distributed among all the possible fixed nitrogen species according to a local thermodynamic equilibrium. The conversion of fixed nitrogen to N_2 can then be described using the known kinetics of reactions 1-5.

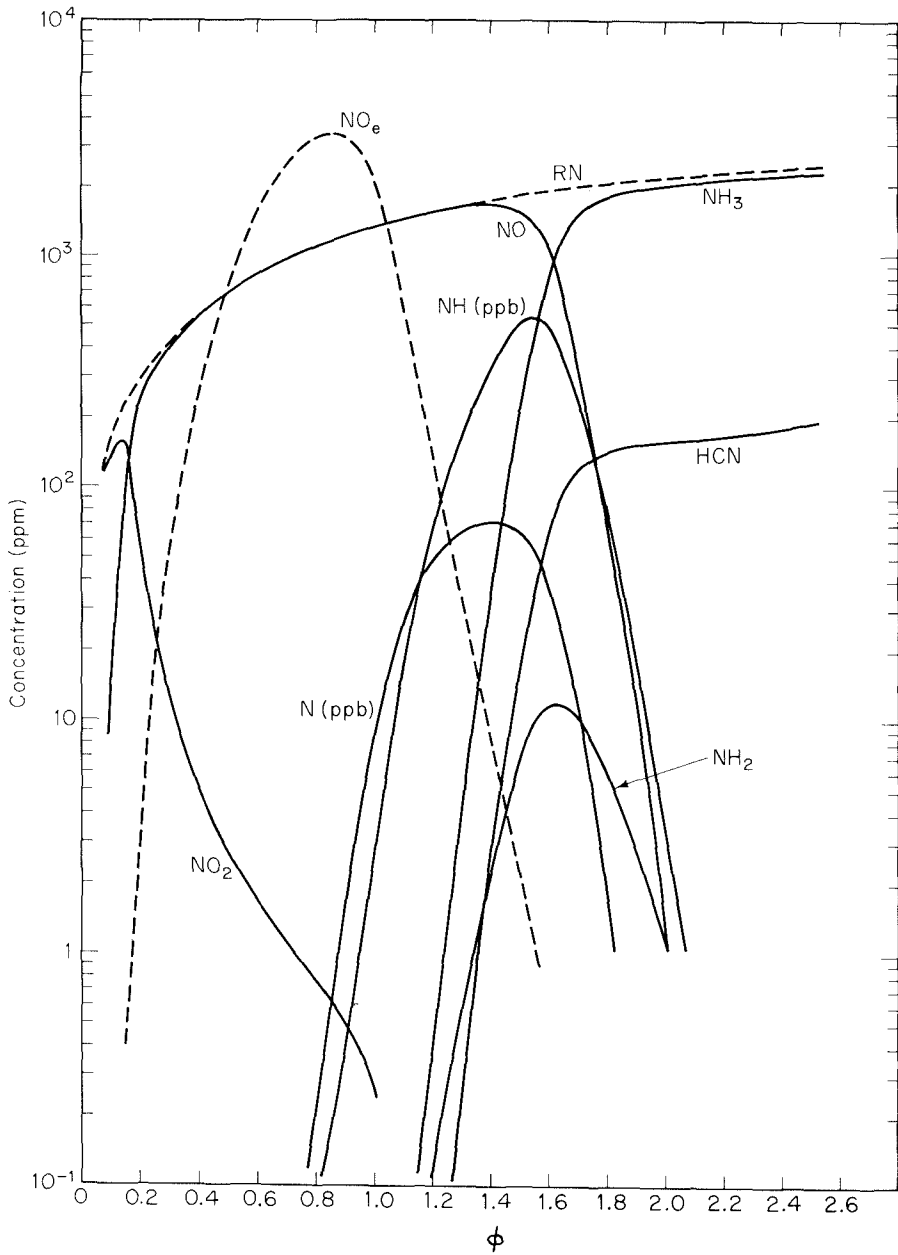


Figure 3.6 Partial equilibrium distribution of single nitrogen species for adiabatic combustion of a fuel oil containing 1% by weight of nitrogen. Total concentration of fixed nitrogen for this fuel and the NO concentration corresponding to full thermodynamic equilibrium are shown by broken lines.

The distribution of fixed nitrogen species in the partial equilibrium is a strong function of equivalence ratio and temperature, but not of the total quantity of fixed nitrogen since the fixed nitrogen is a relatively small component of the fuel. To a first approximation we may assume that in adiabatic combustion the fraction of the fixed nitrogen present in any form is a function of equivalence ratio alone. The partial equilibrium concentration ratios,

$$\begin{aligned}\alpha_{\text{NO}} &= \frac{[\text{NO}]}{[\text{RN}]} \\ \alpha_{\text{N}} &= \frac{[\text{N}]}{[\text{RN}]} \\ \alpha_{\text{NH}} &= \frac{[\text{NH}]}{[\text{RN}]}\end{aligned}\quad (3.19)$$

are thus functions of equivalence ratio, but not of the total concentration of fixed nitrogen, $[\text{RN}] = [\text{NO}] + [\text{N}] + [\text{NH}] + [\text{NH}_2] + [\text{NH}_3] + [\text{CN}] + [\text{HCN}] + [\text{NO}_2]$. A rate equation describing the rate of change in the total amount of fixed nitrogen by all reactions of the type



may now be written in the form

$$\begin{aligned}R_{\text{RN}} &= -2(k_{+1}\alpha_{\text{N}}\alpha_{\text{NO}} + k_{+2}\alpha_{\text{N}}\alpha_{\text{NH}} + k_{+3}\alpha_{\text{NH}}\alpha_{\text{NH}} + k_{+4}\alpha_{\text{NO}}\alpha_{\text{NH}} + k_{+5}\alpha_{\text{NO}}\alpha_{\text{NH}_2})[\text{RN}]^2 \\ &\quad + 2(k_{-1}[\text{O}] + k_{-2}[\text{H}] + k_{-5a}[\text{H}_2\text{O}])[\text{N}_2] + 2k_{-3}[\text{N}_2\text{H}][\text{H}] \\ &\quad + 2k_{-4}[\text{H}][\text{N}_2\text{O}]\end{aligned}\quad (3.20)$$

Based on the study of thermal fixation, the reaction of N_2 with O clearly dominates the fixation of N_2 . We may lump together all of the terms describing N_2 formation into a single rate constant for the reaction of species in the RN pool:

$$\begin{aligned}k_e(\phi, T) &= k_{+1}\alpha_{\text{N}}\alpha_{\text{NO}} + k_{+2}\alpha_{\text{N}}\alpha_{\text{NH}} + k_{+3}\alpha_{\text{NH}}\alpha_{\text{NH}} \\ &\quad + k_{+4}\alpha_{\text{NO}}\alpha_{\text{NH}} + k_{+5}\alpha_{\text{NO}}\alpha_{\text{NH}_2}\end{aligned}\quad (3.21)$$

Figure 3.7 shows how k_e depends on ϕ for the adiabatic combustion conditions of Figure 3.6. The rate constants used in these calculations are summarized in Table 3.1. The total rate (including contributions of reactions 1–5) is shown by the solid lines. Reactions 1 and 5 dominate; their contributions are shown separately by dashed lines. The rate for fuel-lean combustion is too low to remove significant quantities of fixed nitrogen, even where such removal is thermodynamically favored.

In the fuel-rich region where the initial RN concentration is far in excess of equilibrium, only the RN removal term is important, so we may write

$$R_{\text{RN}} = -k_e(\phi, T)[\text{RN}]^2\quad (3.22)$$

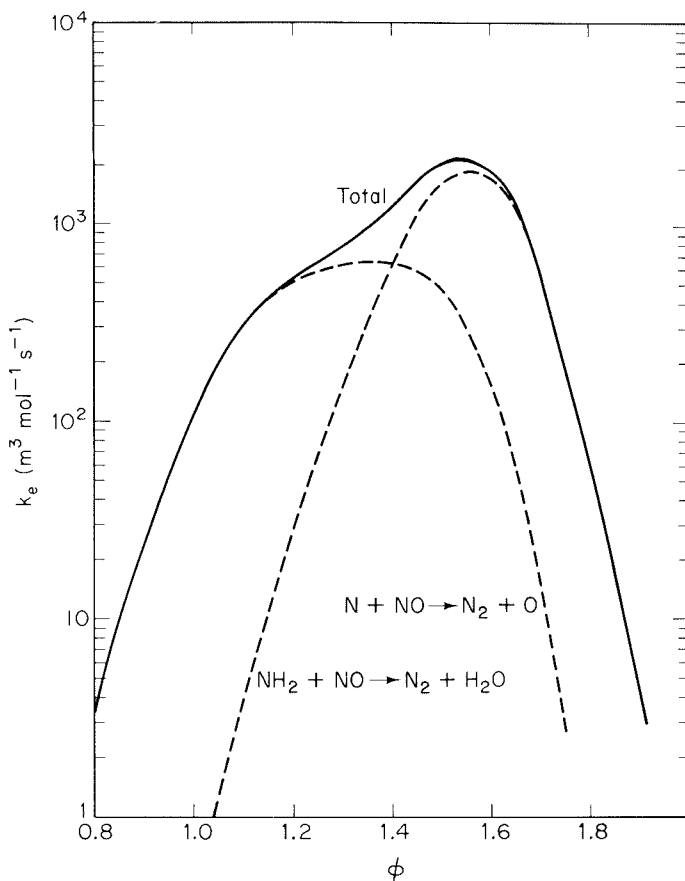


Figure 3.7 Effective reaction rate for the RN + RN reaction.

TABLE 3.1 RATE CONSTANTS FOR THE RN + RN
→ ··· N₂ REACTIONS

Reaction	Rate constant (m ³ mol ⁻¹ s ⁻¹)
$\text{N} + \text{NO} \xrightleftharpoons[-1]{+1} \text{N}_2 + \text{O}$	$k_{+1} = 3.8 \times 10^7 e^{-425/T}$ $k_{-1} = 1.8 \times 10^8 e^{-38.370/T}$
$\text{N} + \text{NH} \xrightleftharpoons[2]{2} \text{N}_2 + \text{H}$	$k_2 = 6.3 \times 10^5 T^{0.5}$
$\text{NH} + \text{NH} \xrightleftharpoons[3]{3} \text{N}_2\text{H} + \text{H}$	$k_3 = 7.9 \times 10^5 T^{0.5} e^{-500/T}$
$\text{NO} + \text{NH} \xrightleftharpoons[4]{4} \text{N}_2\text{O} + \text{H}$	$k_4 = 1.1 \times 10^6 e^{-230/T}$
$\text{NO} + \text{NH}_2 \xrightleftharpoons[5]{5} \text{products}$ $\text{N}_2, \text{N}_2\text{O}$	$k_5 = 1.2 \times 10^{14} T^{-2.46} e^{-938/T}$

Source: Hanson and Salimian (1984).

For an isothermal system, $R_{RN} = d[RN]/dt$. Integrating, we find

$$\frac{[RN]}{[RN]_0} = \frac{1}{1 + t/\tau_{RN}} \tag{3.23}$$

where the characteristic time for RN destruction is defined as

$$\tau_{RN} = \{2k_c(\phi)[RN]_0\}^{-1} \tag{3.24}$$

Since the predominant RN species over a wide range of equivalence ratios ($\phi < 1.6$) is NO, the ratio $[RN]/[RN]_0$ is approximately equal to the fraction of the fuel-nitrogen that is converted to NO (i.e., the NO yield). Flagan et al. (1974) showed that the NO yield for high-temperature fuel-rich combustion is well correlated with (3.23). NO yields at reduced temperatures or in lean combustion, however, were found to be lower than predicted. The discrepancy in the fuel-lean flame is thought to result from accelerated NO formation due to the superequilibrium radical concentrations present in hydrocarbon flames.

We have, so far, assumed that all the reactions not involving N_2 are fast. The conversion of the fuel-nitrogen to HCN in hydrocarbon flames is usually completed too rapidly to be measured by probing the flame. In our discussions of combustion equilibrium we saw that the concentrations of the radicals, H, OH, and O, become small at equivalence ratios much larger than unity. The radical concentrations within the flame may be much higher than the equilibrium levels, but the rate of HCN attack can still be expected to decrease as equivalence ratio increases, making this partial-equilibrium model questionable for very fuel-rich combustion. Reduction in the flame temperature would further reduce the concentrations of these radicals and slow the approach to equilibrium of the fixed nitrogen species.

The degree of conversion of fuel-nitrogen to NO_x ($[NO_x]/[RN]_0$) in combustors without special controls for fuel- NO_x is shown in Figure 3.8. A range of conversion efficiencies is observed for any nitrogen content due, in part, to contributions from ther-

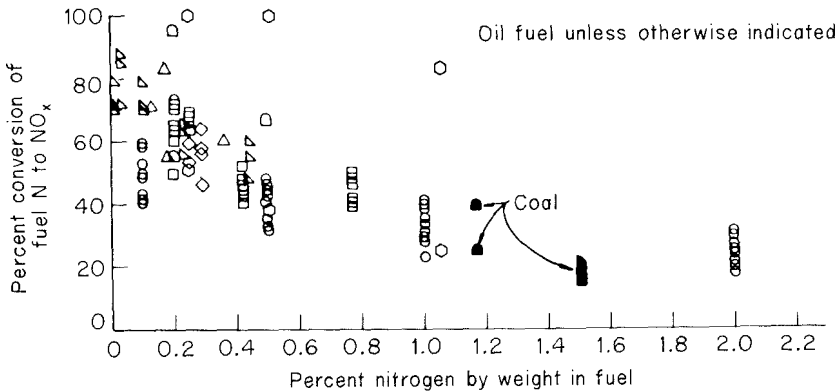


Figure 3.8 Conversion of fuel-nitrogen to NO in a variety of laboratory- and pilot-scale combustors.

mal fixation of N_2 . There is, however, a distinct lower bound to the degree of conversion, and that lower limit to the conversion decreases as the nitrogen content of the fuel increases.

The fuel-nitrogen conversion is lower than one would expect based on the mechanism described above and the overall equivalence ratios (generally less than 1) at which the combustion systems are operated. The formation of N_2 is favored by fuel-rich combustion. This discrepancy is attributed to the influence of mixing on fuel- NO_x formations. Imperfect mixing allows combustion gases to remain fuel-rich even though the combustor is fuel-lean overall, thereby reducing the amount of fuel- NO_x formed.

Figure 3.9 shows the effects of changing mixing rates on the formation of NO_x from combustion of kerosene doped with 0.51% fuel-nitrogen in the same plug flow combustor on which we have focused in our previous discussions of mixing. Once again, high atomizing pressures yield high mixing rates and relatively uniform compositions for the combustion gases. The amount of NO corresponding to 100% conversion of the fuel-nitrogen is shown by the solid line. The dashed line adds to this the quantity of NO formed in well-mixed combustion in the absence of fuel nitrogen, i.e., that due to thermal fixation of N_2 . Consider first the results for well-mixed combustion. NO yields for fuel-lean combustion are close to the amount of fuel-nitrogen and exceed the fuel nitrogen near stoichiometric. The excess NO is due to the thermal fixation of atmospheric nitrogen. As the equivalence ratio is increased beyond unity, the NO level drops rapidly. This we expect from the mechanism described above. As the mixing rate (atomizing pressure) is decreased, the NO yield decreases at all equivalence ratios. At the lowest mixing rates, the NO mole fraction is almost independent of the equivalence ratio.

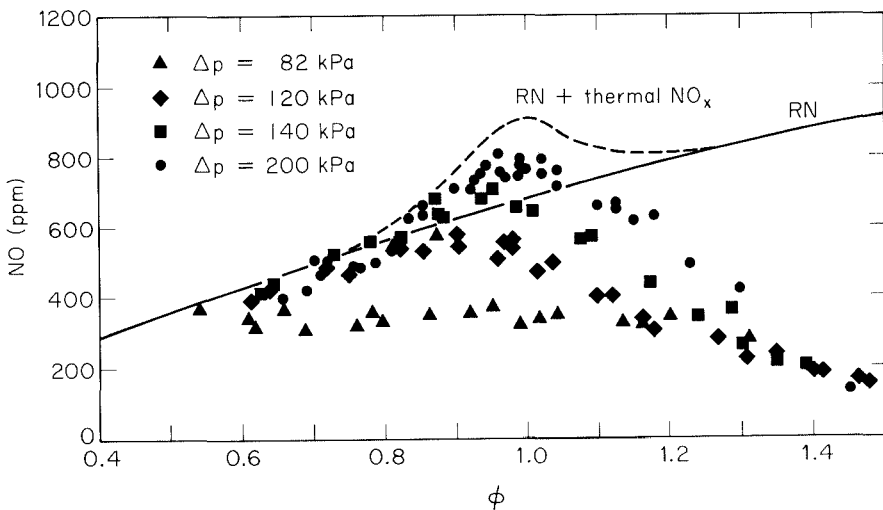


Figure 3.9 Influence of mixing on fuel nitrogen conversion to NO_x . Data are from combustion of kerosene doped with 0.51% nitrogen by weight using an air-assist atomizer (Flagan and Appleton, 1974). Reprinted by permission of The Combustion Institute.

The interaction between turbulent mixing and the chemical kinetics of fuel-nitrogen conversion is too complicated to be treated with the simple probability density function approach that we have applied to thermal fixation and CO concentrations. The length of time a fluid element resides at high equivalence ratios determines the amount of fixed nitrogen that will remain when it is finally diluted with air to substoichiometric conditions. More elaborate descriptions of the evolution of the probability density function in turbulent mixing (e.g., Flagan and Appleton, 1974; Pope, 1985) are needed for calculations of fuel-nitrogen conversion in turbulent flames, but these models are beyond the scope of this book.

The nitrogen in solid or heavy fuel oils may be released with the volatiles and will behave like the volatile nitrogen compounds discussed above, or it may remain with the refractory materials, forming part of the char. In distillation of heavy oils, the nitrogen is generally concentrated in the heavy fractions. Studies of the fate of organically bound nitrogen in coal have shown the char to be slightly enriched in nitrogen (Pohl and Sarofim, 1975). The effect appears to be small, so to a first approximation the fraction of nitrogen in the char may be assumed to be in proportion with the char yield.

The char introduces two factors that we have not yet taken into account. The char particle consumes oxygen, thereby providing a locally reducing atmosphere that can promote the conversion of NO to N₂. Second, there is evidence of NO being reduced on carbon surfaces (Wendt et al., 1979). There are two possible paths for nitric oxide reduction on carbon:

1. Direct reduction to N₂
2. Transformation of NO to HCN or NH₃

The reduced nitrogen species may undergo further reactions on the surface to form N₂. The effective rate of NO reduction on char surfaces has been measured by Levy et al. (1981),

$$R_{\text{NO}} = 4.18 \times 10^4 e^{-17,500/T} p_{\text{NO}} \text{ mol NO m}^{-2} \text{ s}$$

where the rate is based on the exterior surfaces of the char particles. This rate was determined in combustion of char approximately 50 μm in size.

As the char is oxidized, the char-bound nitrogen is released. Since the major reactive gases are O₂ and CO₂, a substantial fraction may be expected to leave the surface as NO, although CN and NH are also possible. Diffusion within the porous structure of the char provides ample opportunity for NO to be reduced by surface reactions in low temperature combustion of large particles, typical of fluidized-bed combustion (Wendt and Schulze, 1976). At the higher temperatures typical of pulverized coal combustion, the release of char nitrogen as NO was found to decrease with increasing particle size. That is to be expected since the atmosphere at the particle surface becomes increasingly reduced as the limit of diffusion-controlled combustion is approached. In fuel-rich pulverized fuel combustion experiments, the NO level is observed to rise rapidly to a maximum and then decay slowly (Wendt et al., 1979). In char combustion, the decline was

attributed to heterogeneous reduction of NO on the char surface. The hydrogen released with the volatile matter from coal increases the concentration of NH_3 , HCN, and other fixed nitrogen species, accelerating the rate of homogeneous conversion of NO to N_2 beyond the heterogeneous reactions. In either case, extended residence times in fuel-rich conditions promote the conversion of fuel-nitrogen to N_2 .

3.1.5 Fuel- NO_x Control

Since the conversion of fuel-nitrogen to NO is only weakly dependent on temperature but is a strong function of the combustion stoichiometry, temperature reduction by flue gas recycle or steam injection, which are effective methods for thermal- NO_x , have little influence on fuel- NO_x . What is required to minimize the amount of fuel-nitrogen leaving a combustor as NO is that the gases be maintained fuel-rich long enough for the N_2 -forming reactions to proceed. Since the overall combustion process must be fuel-lean if high combustion efficiency is to be maintained, this generally requires dividing the combustion process into separate fuel-rich and fuel-lean stages.

A number of names are applied to the various implementations of staged combustion, including: overfire air, off-stoichiometric combustion, and low- NO_x burners. Most commonly, only part of the air required for complete combustion is supplied with the fuel. The remaining air is supplied through separate "overfire air" ports. Staged combustion was first applied to the control of thermal- NO_x because it allowed some of the heat to be rejected before completing the combustion process, but it is better suited to fuel- NO_x control since it provides the time required for N_2 formation. This can be carried too far, however. If the primary combustion zone is operated too fuel-rich, the fixed nitrogen can be retained in a combustible form (e.g., HCN). When the secondary air is added, such compounds may act as fuel-N and form NO_x rather than the N_2 that was sought. The NO_x emissions from staged combustors, as a result, may pass through a minimum as the equivalence ratio of the primary combustion zone is increased.

The "low- NO_x " burners, illustrated in Figure 3.10, utilize burner aerodynamics to slow the rate at which fuel and air are mixed. Whereas most burners are designed to achieve a highly turbulent zone of intense combustion, the low- NO_x burners are designed to produce a long, "lazy" flame. The degree of control that can be reached by this method is limited by the need to achieve complete combustion within the volume of the combustor. Low- NO_x burners have the important advantage of being a relatively low cost technology that can be used as a retrofit on existing sources to reduce NO_x emissions.

3.1.6 Postcombustion Destruction of NO_x

Reactions similar to those that convert fixed nitrogen to N_2 in combustion can be used to destroy nitrogen oxides in the postflame gases. Because of the similarity of these processes to combustion, we shall discuss these postcombustion treatment methods here rather than in the chapter on gas cleaning.

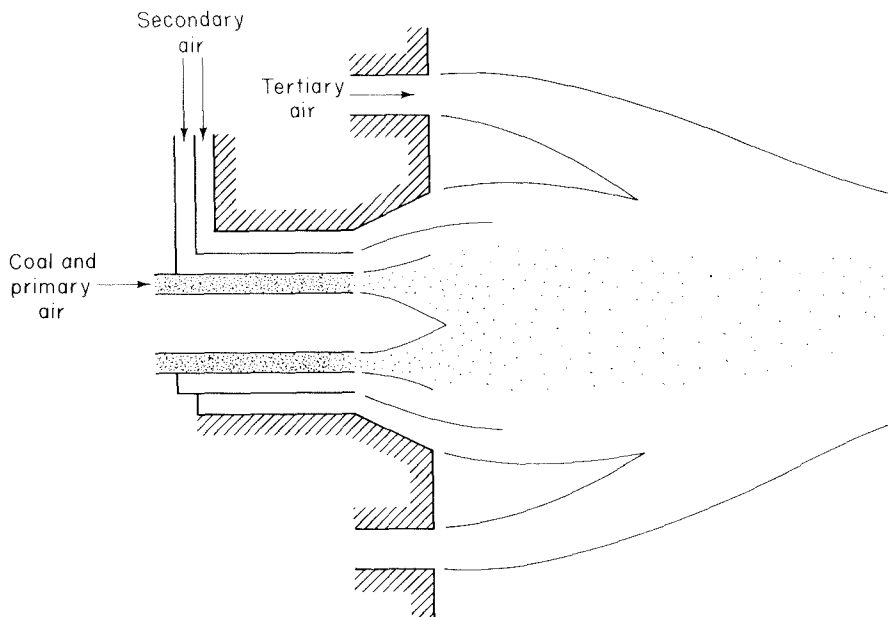


Figure 3.10 Coal burner designed to reduce formation of NO_x by spreading the mixing of fuel and air.

Wendt et al. (1973) demonstrated that nitrogen oxides could be reduced, presumably to N_2 , by injection and oxidation of fuel in the partially cooled combustion products. This method takes advantage of the shift in the equilibrium NO concentration associated with the temperature reduction. The NO formed in the high-temperature flame region is generally not reduced as the equilibrium level decreases due to the low concentration of nitrogen atoms. When a fuel such as methane is added at sufficiently high temperature (e.g., 1800 K), it is oxidized, generating high concentrations of radicals. These radicals promote the formation of N and other reactive fixed nitrogen species from NO , for example,

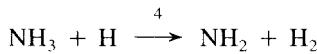
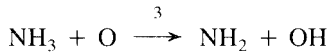
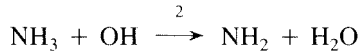
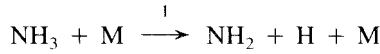


These species then react with NO to form N_2 .

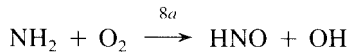
At lower temperatures, selective reduction of NO by fixed nitrogen species (e.g., NH_3) may be used to destroy NO_x in the products of combustion, even in the presence of a large excess of oxygen (Wendt et al., 1973; Lyon, 1976; Muzio et al., 1979). The noncatalytic process using ammonia is called the thermal de- NO_x process. The temperature range in which the reaction between NH_i species and NO is favored over the formation of additional NO (i.e., less than 1500 K) is much lower than typical flame temperatures.

Several detailed studies of the kinetics and mechanisms of selective reduction of NO by ammonia have been reported (Branch et al., 1982; Miller et al., 1981; Lucas and Brown, 1982; Dean et al., 1982). The partial-equilibrium assumption used in the dis-

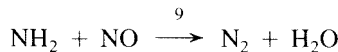
cussion of fuel-NO_x is not valid at such low temperatures since the endothermic reverse reactions are too slow to maintain the equilibrium among the single nitrogen species. The NH₃ does not react directly with the NO. Before any NO can be reduced to N₂, the ammonia must decompose by reactions such as



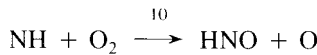
The NH₂ may undergo further oxidation, that is,



Alternatively, the NH₂ may react with NO, leading to the ultimate formation of N₂,

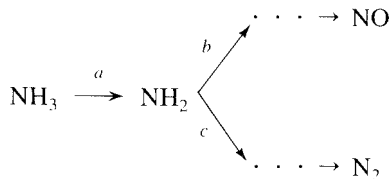


The NH produced by reactions 5-7 is highly reactive and can be attacked by O₂ with a low activation energy:



forming the NO bond. Thus, once the NH₂ is oxidized, the formation of NO or related species quickly follows.

The overall reaction sequence may be written



The rate equations may be written in terms of the characteristic times of each of the three types of reactions:

$$R_{\text{NH}_3} = -\frac{[\text{NH}_3]}{\tau_a} \quad (3.25)$$

$$R_{\text{NH}_2} = \frac{[\text{NH}_3]}{\tau_a} - \frac{[\text{NH}_2]}{\tau_b} - \frac{[\text{NH}_2][\text{NO}]}{\tau_c[\text{NO}]_0} \quad (3.26)$$

$$R_{\text{NO}} = \frac{[\text{NH}_2]}{\tau_b} - \frac{[\text{NH}_2][\text{NO}]}{\tau_c[\text{NO}]_0} \quad (3.27)$$

where the characteristic reaction times are defined by

$$\tau_a^{-1} = k_1[\text{M}] + k_2[\text{OH}] + k_3[\text{O}] + k_4[\text{H}] \quad (3.28)$$

$$\tau_b^{-1} = k_5[\text{OH}] + k_6[\text{O}] + k_7[\text{H}] + k_8[\text{O}_2] \quad (3.29)$$

$$\tau_c^{-1} = k_9[\text{NO}]_0 \quad (3.30)$$

Since we are dealing with combustion products that have generally had several seconds to equilibrate, a reasonable first approximation to the concentrations of the radicals OH, O, and H is that chemical equilibrium is achieved. The NO and added NH₃ are minor species, so their effect on the equilibrium composition should be small. Restricting our consideration to an isothermal system, the density and radical concentrations are constant, and we may integrate (3.25) to find

$$[\text{NH}_3] = [\text{NH}_3]_0 e^{-t/\tau_a} \quad (3.31)$$

We immediately see one of the limitations to the use of ammonia injection for NO_x control. If the rates of the ammonia reactions are too slow due to low temperature, the ammonia will be emitted unreacted along with the nitric oxide.

Once NH₂ is produced, it will react rapidly, either with radicals or with NO. If we assume that these reactions are sufficiently fast to establish a steady state, the NH₂ concentration may be estimated as

$$[\text{NH}_2]_{ss} = \frac{([\text{NH}_3]_0/\tau_a) e^{-t/\tau_a}}{(1/\tau_b) + ([\text{NO}]/[\text{NO}]_0)(1/\tau_c)} \quad (3.32)$$

We now have the estimates of the concentrations of NH₂ and NH₃ that we need to determine the NO levels. It is convenient to define the following dimensionless quantities:

$$z = \frac{[\text{NO}]}{[\text{NO}]_0}$$

$$\chi = \frac{[\text{NH}_3]_0}{[\text{NO}]_0}$$

$$\theta = \frac{t}{\tau_a}$$

$$\gamma = \frac{\tau_b}{\tau_c}$$

The rate equation for the NO concentration in an isothermal system becomes

$$\frac{dz}{d\theta} = \frac{1 - \gamma z}{1 + \gamma z} \chi e^{-\theta} \quad (3.33)$$

The initial condition is $z = 1$ at $\theta = 0$. Integrating, we find

$$1 - z - \frac{2}{\gamma} \ln \frac{1 - \gamma z}{1 - \gamma} = \chi(1 - e^{-\theta}) \quad (3.34)$$

Equation (3.34) may be solved iteratively to determine the level of NO control in the selective reduction system. Fig 3.11 compares the results of these calculations with measurements made by Muzio and Arand (1976) on a pilot-scale facility. The rate constants used in this calculation are summarized in Table 3.2. The calculations are based on a 0.35-s residence time in an isothermal system. In the test facility the temperature decreased by about 200 K within this time. The reported temperatures correspond approximately to the temperature at the point where the ammonia was injected. The radical concentrations and reaction rates will decrease as the gases cool, so our simple model is not strictly valid.

Nevertheless, this simple model reproduces most of the important features of the selective reduction system. NO is effectively reduced only in a narrow temperature window centered about 1200 K. As shown in Figure 3.11(c), θ is small at lower temperatures due to the slow reaction of ammonia. At higher temperatures, the NH_2 oxidation becomes faster than NO reduction (i.e., $\gamma > 1$), as shown in Figure 3.11(c), allowing additional NO to be formed from the ammonia. Even when excess ammonia is added near the optimal temperature, not all of the nitric oxide is reduced since some of the NH_3 forms NO.

It is apparent in Figure 3.11 that this model predicts a much broader temperature window than was observed experimentally. The high-temperature limit of the window is reproduced reasonably well. The model, however, predicts that NH_3 is oxidized more rapidly than is observed at low temperatures. The primary oxidation reaction is reaction 2:



An overestimate of the hydroxyl concentration due to ignoring the temperature variation along the length of the experimental section could account for much of the discrepancy.

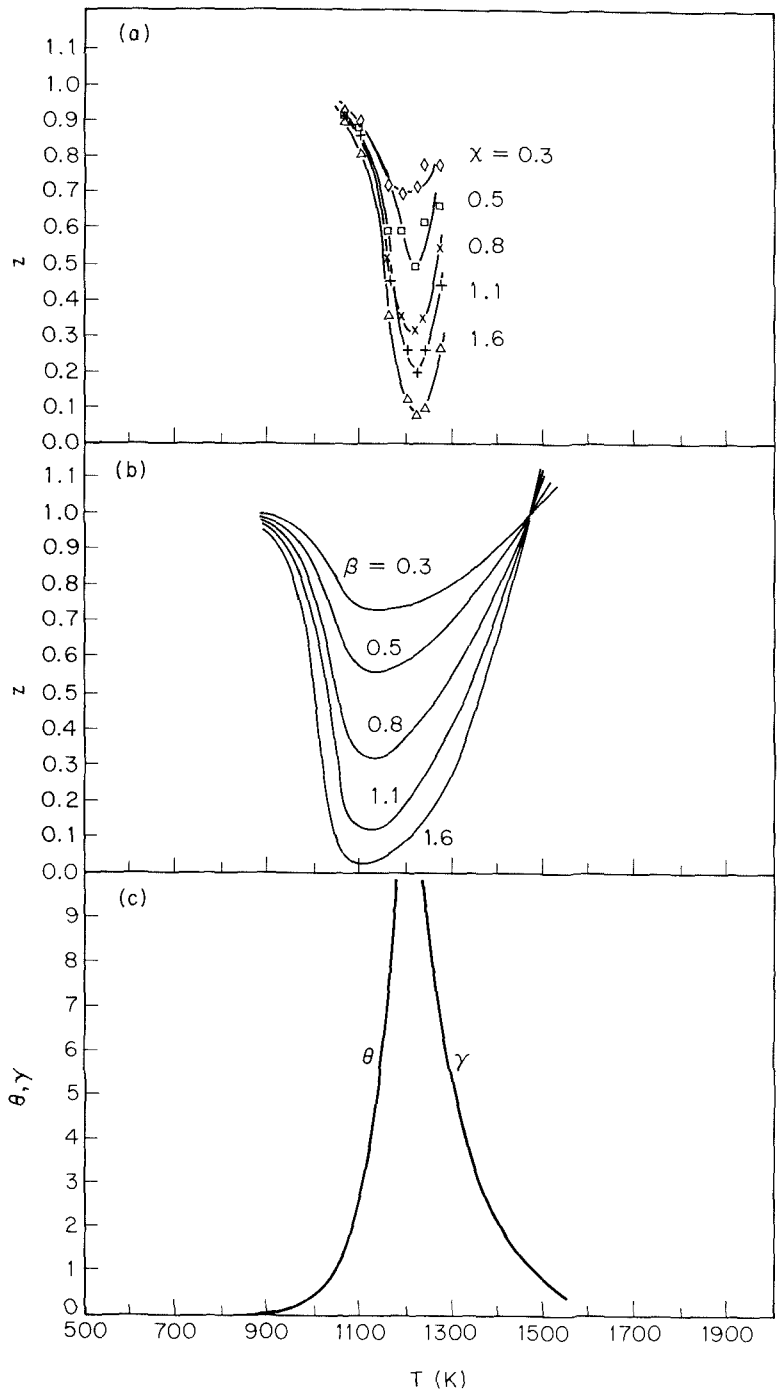


Figure 3.11 Performance of ammonia injection in the destruction of NO_x in combustion products: (a) NO_x penetration data of Muzio and Arand (1976); (b) calculated NO penetration; (c) dimensionless times for NH_3 and NH_2 oxidation.

TABLE 3.2 RATE CONSTANTS FOR THE NH₃/NO REACTIONS

Reaction	Rate constant (m ³ mol ⁻¹ s ⁻¹)
NH ₃ + M $\xrightarrow{1}$ NH ₂ + H + M	$k_1 = 2.5 \times 10^{10} e^{-47.200/T}$
NH ₃ + OH $\xrightarrow{2}$ NH ₂ + H ₂ O	$k_2 = 5.8 \times 10^7 e^{-4055/T}$
NH ₃ + O $\xrightarrow{3}$ NH ₂ + OH	$k_3 = 2.0 \times 10^7 e^{-4470/T}$
NH ₃ + H $\xrightarrow{4}$ NH ₂ + H ₂	$k_4 = 1.3 \times 10^8 e^{-10.280/T}$
NH ₂ + OH $\xrightarrow{5}$ NH + H ₂ O	$k_5 = 5.0 \times 10^5 T^{0.5} e^{-1000/T}$
NH ₂ + O $\xrightarrow{6a}$ NH + OH	$k_{6a} = 1.3 \times 10^8 T^{-0.5}$
$\xrightarrow{6b}$ HNO + H	$k_{6b} = 6.3 \times 10^8 T^{-0.5}$
NH ₂ + H $\xrightarrow{7}$ NH + H ₂	$k_7 = 1.9 \times 10^7$
NH ₂ + O ₂ $\xrightarrow{8a}$ HNO + OH	$k_{8a} = 10^8 e^{-25.000/T}$
$\xrightarrow{8b}$ NH + HO ₂	$k_{8b} = 1.8 \times 10^6 e^{-7500/T}$
NH ₂ + NO $\xrightarrow{9}$ N ₂ + H ₂ O	$k_9 = 1.2 \times 10^{14} T^{-2.46} e^{-938/T}$
NH + O ₂ $\xrightarrow{10}$ HNO + O	$k_{10} = 10^7 e^{-6000/T}$

Source: Hanson and Salimian (1984).

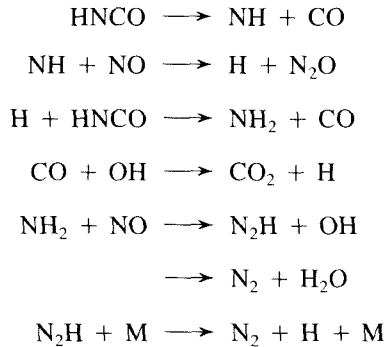
The extreme temperature sensitivity of the NH₃-NO reaction mechanism makes the location of the ammonia injection extremely important. The temperature window corresponds to the gas temperature in boiler superheaters and convective heat exchangers where the temperature drops rapidly. The temperature at a given point in a boiler also changes with load. If the location of the injectors were optimized for full-load operation, the temperature would drop at reduced load. Instead of reducing NO, the ammonia would then be emitted into the atmosphere. Optimizing for a lower load condition would allow ammonia oxidation when the temperature increases at full load. One way around this problem is to use injectors at multiple locations, although the heat exchangers limit the locations of the injectors, particularly when an existing boiler is being retrofitted with the control.

The original implementation of selective reduction was based on ammonia, but the narrow-temperature window severely limits the range of systems to which it can be applied. Major efforts have been undertaken to elucidate the chemistry involved, with the ultimate objective of making the temperature restrictions less severe. One approach is to use catalysts to promote the reaction at lower temperatures, but catalyst poisoning by contaminants like ash in the combustion products presents major obstacles to this approach. Alternatively, a radical source could reduce the lower bound of the temperature window. Salimian and Hanson (1980) found that the optimal temperature for the ammonia reaction could be reduced to about 1000 K by adding hydrogen along with the ammonia. Azuhata et al. (1981) observed that H₂O₂ could promote the NH₃ reaction at temperatures as low as 800 K.

The essence of the selective reduction technique is the introduction of nitrogen compounds that will react with NO, leading to the ultimate formation of N₂. The temperature at which the reaction proceeds must be slow enough that NO formation from the additive is avoided. Compounds other than ammonia have been proposed. Urea, H₂NCONH₂, lowers the temperature window to approximately 1000 K (Salimian and Hanson, 1980). Other compounds look even more promising. Perry and Siebers (1986) have found that isocyanic acid is extremely effective at reducing NO at temperatures as low as 670 K. Isocyanic acid was produced by flowing hot combustion products over a bed of cyanic acid which undergoes thermal decomposition at temperatures in excess of 600 K,



The combustion products were then passed over a bed of stainless steel pellets. Their proposed mechanism for the reactions within the packed bed is

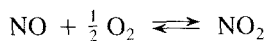


At sufficiently low temperature, the gas-phase NO formation is avoided, but surface reactions of oxygen in the bed may lead to NO formation. Above about 670 K, very low NO_x levels were observed in tests on a diesel engine. Thus promising technologies for reducing NO in the combustion products are under development.

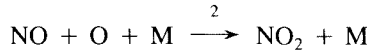
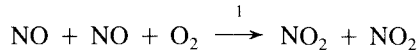
3.1.7 Nitrogen Dioxide

Most of the nitrogen oxides emitted from combustion systems are in the form of nitric oxide (NO), but nitrogen dioxide (NO₂) is usually present as well. In the combustion zone, NO₂ levels are usually low, but exhaust levels can be significant at times. NO₂ can account for as much as 15 to 50% of the total NO_x emitted by gas turbines (Diehl, 1979; Hazard, 1974; Levy, 1982). NO₂ levels far in excess of the NO concentration have been measured in some regions of laminar diffusion flames (Hargreaves et al., 1981).

Nitrogen dioxide is formed by the oxidation of NO. The overall reaction for the process is



which is exothermic [i.e., $\Delta h_r(298 \text{ K}) = -57,278 \text{ J mol}^{-1}$]. Thus the formation of NO_2 is thermodynamically favored at low temperatures. The fact that NO_2 is usually much less abundant than NO in cooled combustion products clearly indicates that the rate of NO oxidation is a relatively slow process. The overall reactions of NO with O_2 or O are termolecular

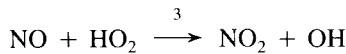


for which the measured rate constants are (Baulch et al., 1973)

$$k_{+1} = 1.2 \times 10^{-3} \exp\left(\frac{530}{T}\right) \quad \text{m}^6 \text{ mol}^{-2} \text{ s}^{-1}$$

$$k_{+2} = 1.5 \times 10^3 \exp\left(\frac{940}{T}\right) \quad \text{m}^6 \text{ mol}^{-2} \text{ s}^{-1}$$

The conversion of NO to NO_2 by the hydroperoxyl radical



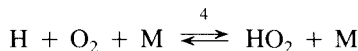
with a rate constant (Hanson and Salimian, 1984)

$$k_{+3} = 2.1 \times 10^6 \exp\left(\frac{240}{T}\right) \quad \text{m}^3 \text{ mol}^{-1} \text{ s}^{-1}$$

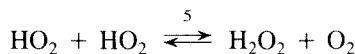
is generally slow because HO_2 is present only at low concentrations, at least as long as equilibrium of the C-H-O system is maintained. Within the flame front, superequilibrium radical concentrations can lead to some NO_2 formation, but NO_2 dissociation by the reverse of reaction 2 is likely if it passes through the hot region of the flame,

$$k_{-2} = 1.1 \times 10^{10} \exp\left(-\frac{33,000}{T}\right) \quad \text{m}^3 \text{ mol}^{-1} \text{ s}^{-1}$$

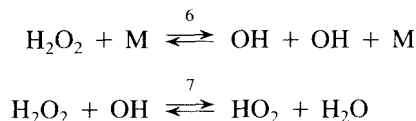
High NO_2 levels are observed following rapid cooling of combustion products (Hargreaves et al., 1981). While HO_2 is a relatively minor species in the flame, relatively high concentrations can be formed by the three-body recombination reaction



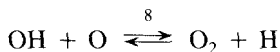
in regions where fuel-lean combustion products are rapidly cooled, accelerating NO_2 formation in the cool gases. Reactions of HO_2 with major species (CO , H_2 , O_2 , etc.) are slow at low temperatures. It does, however, react with NO via reaction 3 and with itself.



The H_2O_2 produced by reaction 5 is stable at low temperature, but at higher temperatures may react further,



regenerating HO_2 and minimizing the effect of reaction 5. Bimolecular exchange reactions of OH, for example,

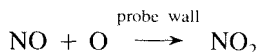


generate the H necessary for reaction 4.

Reactions 3–8 can explain substantial conversion of NO to NO_2 that is observed when combustion products are rapidly cooled to intermediate temperatures, on the order of 1000 K (Hargreaves et al., 1981). A detailed treatment of NO_2 formation requires an understanding of the rates of destruction of the radicals in combustion products. The radicals are ultimately consumed by three-body recombination reactions. Since these reactions are relatively slow, rapid cooling can allow substantial radical concentrations to remain at the low temperatures where NO_2 is stable. Slower cooling would allow the radicals to remain equilibrated to lower temperature, thereby eliminating the conditions necessary for fast NO oxidation. A detailed treatment of this radical chemistry in cooled combustion products will be presented as part of our discussion of CO oxidation.

The foregoing analysis clearly indicates that NO_2 formation is favored by rapid cooling of combustion products in the presence of substantial O_2 concentrations. Gas turbine engines provide such conditions due to the need to limit the temperatures of the combustion products entering the power turbine. Stable combustion requires near stoichiometric operation that yields temperatures much higher than the tolerable (< 1400 K) turbine inlet temperatures. To cool the combustion products to this temperature, additional air is injected downstream of the primary combustion zone. This reduces the overall equivalence ratio to 0.2 to 0.4 and provides abundant oxygen for HO_2 formation. Since engine size is a premium in aircraft gas turbines, the residence time is kept very short, of order 10 ms, providing the rapid quenching needed to favor NO_2 formation.

To measure the composition of gas samples extracted from flames, it is necessary to cool the gases rapidly to quench the oxidation of CO and other species. Rapid cooling in sample probes also provides the conditions that favor NO_2 formation (Cernansky and Sawyer, 1975; Allen, 1975; Levy, 1982). A rapid quench sample probe also provides a large surface that can catalyze the recombination reaction

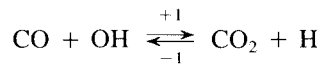


Some of the early reports of high NO_2 levels in flames were plagued by probe-induced sampling biases. A better understanding of the kinetics of NO_2 formation has made it possible to minimize probe sampling biases in in-flame studies. Estimates of NO_2 levels in flames have decreased accordingly.

3.2 CARBON MONOXIDE

In Chapter 2 we saw that carbon monoxide is an intermediate species in the oxidation of hydrocarbon fuels to CO_2 and H_2O . In fuel-rich regions of a flame, the CO levels are necessarily high since there is insufficient oxygen for complete combustion. Only if sufficient air is mixed with such gases at sufficiently high temperature can the CO be oxidized. Thus, imperfect mixing can allow carbon monoxide to escape from combustors that are operated fuel-lean overall. Even in premixed combustion systems, carbon monoxide levels can be relatively high due to the high equilibrium concentrations at the flame temperature, particularly in internal combustion engines where the gases are hot prior to ignition due to compression. As the combustion products are cooled by heat or work transfer, the equilibrium CO level decreases. If equilibrium were maintained as the temperature decreased, carbon monoxide emissions from automobiles and other well-mixed combustors would be very low in fuel-lean operation. The extent to which CO is actually oxidized, however, depends on the kinetics of the oxidation reactions and the manner of cooling. In this section we explore the kinetics of CO oxidation and the mechanisms that allow CO to escape oxidation in locally fuel-lean combustion.

The predominant reaction leading to carbon monoxide oxidation in hydrocarbon combustion is



where

$$k_{+1} = 4.4 T^{1.5} e^{372/T} \quad \text{m}^3 \text{mol}^{-1} \text{s}^{-1}$$

The rate of carbon dioxide production by reaction 1 is

$$R_{+1} = k_{+1}[\text{CO}][\text{OH}]$$

The rate equation describing the total change in the CO level must include the reverse reactions:

$$\begin{aligned} R_{\text{CO}} &= -R_{+1} + R_{-1} \\ &= -k_{+1}[\text{CO}][\text{OH}] + k_{-1}[\text{CO}_2][\text{H}] \end{aligned}$$

where, by detailed balancing,

$$k_{-1} = \frac{k_{+1}}{K_{c1}}$$

Thus, to describe the CO oxidation kinetics, we must know the concentrations of OH and H.

In this discussion, our primary concern is the oxidation of CO in the postflame gases as they cool. The speed of the reactions in responding to a perturbation from the equilibrium state may be expressed in terms of the characteristic reaction time,

$$\tau_{\text{CO}} = \frac{[\text{CO}]}{R_{+1}} = \frac{1}{k_{+1}[\text{OH}]}$$

As a first approximation, the OH may be assumed to be present at its equilibrium concentration. The dotted line in Figure 3.12 shows the variation of τ_{CO} with equivalence ratio as calculated using the results of the combustion equilibrium calculations from Figure 2.6 for adiabatic combustion of a fuel oil ($\text{CH}_{1.8}$). At equivalence ratios greater than about 0.6, corresponding to temperatures greater than 1650 K, the reaction time is less than 1 ms, indicating that the CO level can quickly respond to changes in the equilibrium state of the system. At equivalence ratios below about 0.4 ($T < 1250$ K), the reaction time exceeds 1 s, so chemical equilibrium will be very difficult to maintain in

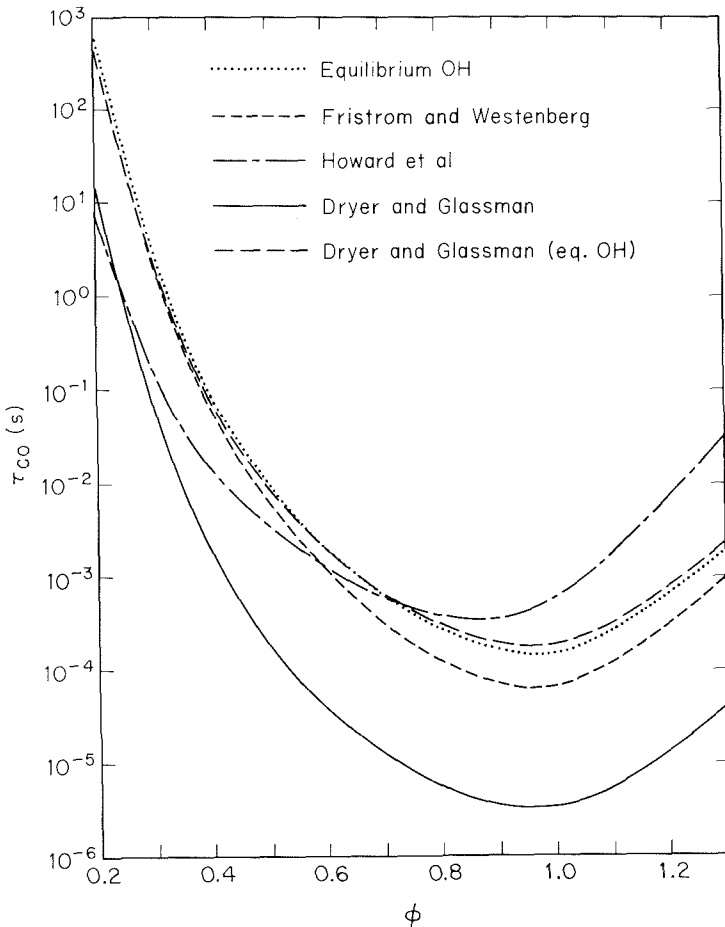
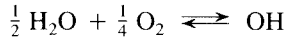


Figure 3.12 Variation of the characteristic time for CO oxidation with equivalence ratio for various global rate expressions.

any combustion system. In the discussion to follow, we show that temperature has the predominant influence on the oxidation rate.

This simple approach to describing CO oxidation can readily be used to derive a global rate expression that will make it possible to estimate oxidation rates without resorting to elaborate chemical equilibrium calculations. The equilibration of OH with H₂O and O₂ can be described by the reaction



giving the equilibrium concentration

$$[\text{OH}]_e = K_{c,\text{OH}}[\text{H}_2\text{O}]^{1/2}[\text{O}_2]^{1/4} \tag{3.35}$$

Similarly, the H concentration may be estimated by assuming equilibrium of the reaction



leading to

$$[\text{H}]_e = K_{c,\text{H}}[\text{H}_2\text{O}]^{1/2}[\text{O}_2]^{-1/4} \tag{3.36}$$

The rate equation for CO thus becomes

$$R_{\text{CO}} = -k_f[\text{CO}][\text{H}_2\text{O}]^{1/2}[\text{O}_2]^{1/4} + k_r[\text{CO}_2][\text{H}_2\text{O}]^{1/2}[\text{O}_2]^{-1/4} \tag{3.37}$$

where $k_f = k_{+1}K_{c,\text{OH}}$ and $k_r = k_{-1}K_{c,\text{H}}$ are the global rate constants. Several investigators have reported global CO oxidation rates in this form (Table 3.3). The first rate expression was fitted to measured CO oxidation rates in postflame gases. The second was derived using the measured rate for reaction 1 and the equilibrium assumption for OH. These two rates agree closely with the calculations made using an equilibrium code to determine $[\text{OH}]_e$, as illustrated by the reaction times shown in Figure 3.12. The third rate expression was derived by fitting CO oxidation data obtained from measurements made in flames. The resulting reaction times are two orders of magnitude shorter than those for equilibrium OH, as illustrated in Figure 3.12. This discrepancy results from superequilibrium OH concentrations within the flame front and clearly indicates the need for caution in applying global reaction rates. Although they may be very useful, the

TABLE 3.3 GLOBAL CO OXIDATION RATE EXPRESSIONS $-R_{\text{CO},ox}$ (mol m⁻³ s⁻¹)

	Temperature range (K)	Reference
(1) $1.3 \times 10^9 [\text{CO}][\text{H}_2\text{O}]^{1/2}[\text{O}_2]^{1/4} \exp(-22,660/T)$	1750–2000	Fristrom and Westenberg (1965)
(2) $1.3 \times 10^7 [\text{CO}][\text{H}_2\text{O}]^{1/2}[\text{O}_2]^{1/2} \exp(-15,100/T)$	840–2360	Howard et al. (1973)
(3) $1.3 \times 10^{10} [\text{CO}][\text{H}_2\text{O}]^{1/2}[\text{O}_2]^{1/4} \exp(-20,140/T)$	1030–1230	Dryer and Glassman (1973)
(4) $1.3 \times 10^8 [\text{CO}][\text{H}_2\text{O}]^{1/2}[\text{O}_2]^{1/4} \exp(-19,870/T)$	Equilibrium OH	Dryer and Glassman (1973)

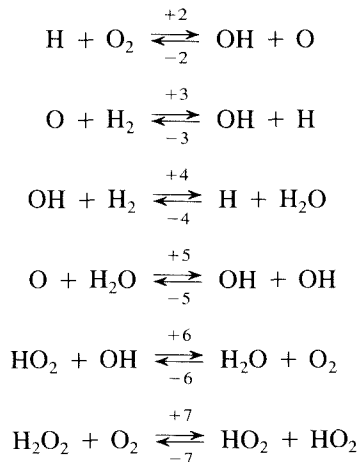
assumptions implicit in global rate expressions sometimes severely limit the range of conditions to which they are applicable.

From these global rate expressions, we can see that the dependence of reaction times on the equivalence ratio is primarily a temperature effect. Since the rate coefficient for the CO + OH reaction is not strongly dependent on temperature at low temperatures, this temperature dependence arises primarily from the influence of temperature on the equilibrium OH concentration. While the influence of temperature on the CO + OH reaction rate is minor, other reactions with larger activation energies are more strongly affected. The reactions involved in the equilibration of hydroxyl and other minor species with the major species include a number with large activation energies. We expect, therefore, that at some point as the gases are cooled the radical concentrations will begin to deviate from chemical equilibrium. This reaction quenching strongly influences the CO oxidation rate and must be taken into consideration.

3.2.1 Carbon Monoxide Oxidation Quenching

While it is beyond the scope of this book to undertake detailed kinetic modeling of the postflame reactions, it is useful to examine the process of reaction quenching qualitatively. Fenimore and Moore (1974) analyzed the problem of CO oxidation quenching in a constant-pressure system. Their analysis allows one to derive an expression for the maximum cooling rate beyond which CO oxidation reactions will be frozen.

As we have noted previously, the radicals O, OH, H, and HO₂ and other reaction intermediates (e.g., H₂ and H₂O₂) undergo a number of rapid exchange reactions, for example,



We must describe the dynamics of these reaction intermediates to determine the instantaneous OH concentration and calculate the rate of CO oxidation.

The exchange reactions are fast compared to the three-body recombination reac-

tions that ultimately eliminate the radicals from the system. To a first approximation the reaction intermediates H, O, OH, HO₂, and H₂ may be assumed to be equilibrated with one another by the action of reactions 2-7. These partial-equilibrium concentrations may be expressed in terms of the hydroxyl concentration as follows:

$$\begin{aligned}
 [\text{O}]_{pe} &= \frac{[\text{OH}]^2}{K_5[\text{H}_2\text{O}]} \\
 [\text{H}]_{pe} &= \frac{[\text{OH}]^3}{K_2K_5[\text{O}_2][\text{H}_2\text{O}]} \\
 [\text{HO}_2]_{pe} &= \frac{[\text{H}_2\text{O}][\text{O}_2]}{K_6[\text{OH}]} \\
 [\text{H}_2]_{pe} &= \frac{[\text{OH}]^2}{K_2K_4K_5[\text{O}_2]} \\
 [\text{H}_2\text{O}_2]_{pe} &= \frac{[\text{H}_2\text{O}]^2[\text{O}_2]}{K_6^2K_7[\text{OH}]^2}
 \end{aligned} \tag{3.38}$$

where all the equilibrium constants are in concentration units (K_c). Using the expression for $[\text{H}]_{pe}$, the rate of CO oxidation may be written

$$R_{\text{CO}} = -k_{+1}[\text{OH}]([\text{CO}] - [\text{CO}]_{pe}) \tag{3.39}$$

where

$$[\text{CO}]_{pe} = \frac{[\text{CO}_2][\text{OH}]^2}{K_1K_2K_5[\text{O}_2][\text{H}_2\text{O}]} \tag{3.40}$$

is the CO concentration corresponding to a partial equilibrium with this pool of reaction intermediates.

The instantaneous rate of CO oxidation is proportional to the hydroxyl concentration, which, in turn, depends on the rate at which OH is consumed. The variation of the ratio, $[\text{CO}]/[\text{CO}]_{pe}$, with $[\text{OH}]$ can be used to identify conditions that lead to deviations from the partial equilibrium.

The ratio, $[\text{CO}]/[\text{CO}]_{pe}$, depends on both the hydroxyl concentration and time. Taking the total derivative with respect to $[\text{OH}]$,

$$\frac{d([\text{CO}]/[\text{CO}]_{pe})}{d[\text{OH}]} = -\frac{[\text{CO}]}{[\text{CO}]_{pe}^2} \frac{d[\text{CO}]_{pe}}{d[\text{OH}]} + \frac{1}{[\text{CO}]_{pe}} \frac{d[\text{CO}]/dt}{d[\text{OH}]/dt}$$

and applying (3.39) and (3.40), we find

$$\alpha[\text{OH}] \frac{d([\text{CO}]/[\text{CO}]_{pe})}{d[\text{OH}]} = (1 - 2\alpha) \frac{[\text{CO}]}{[\text{CO}]_{pe}} - 1 \tag{3.41}$$

where

$$\alpha = \frac{-d[\text{OH}]/dt}{k_1[\text{OH}]^2} \quad (3.42)$$

The value of α determines whether CO will remain equilibrated with the other trace species. If $\alpha = 0$, $[\text{CO}]/[\text{CO}]_{pe} = 1$ and CO is equilibrated with the pool of reaction intermediates. For $\alpha \rightarrow \infty$,

$$\frac{d([\text{CO}]/[\text{CO}]_{pe})}{d[\text{OH}]} = -\frac{2}{[\text{OH}]} \frac{[\text{CO}]}{[\text{CO}]_{pe}}$$

or

$$\frac{[\text{CO}]}{[\text{CO}]_{pe}} \propto [\text{OH}]^{-2}$$

Since $[\text{CO}]_{pe} \propto [\text{OH}]^2$, CO is independent of OH and, therefore, strictly frozen.

For $[\text{CO}]/[\text{CO}]_{pe}$ to be greater than but decreasing toward unity as $[\text{OH}]$ decreases, α must be between 0 and $\frac{1}{2}$. Thus, only if $\alpha < \frac{1}{2}$ can the CO partial equilibrium be continuously maintained. When CO oxidation is quenched, $[\text{CO}]/[\text{CO}]_{pe} \gg 1$; so (3.41) becomes, approximately,

$$\frac{\alpha[\text{OH}]d([\text{CO}]/[\text{CO}]_{pe})}{d[\text{OH}]} = \frac{[\text{CO}]}{[\text{CO}]_{pe}} (1 - 2\alpha)$$

Noting that

$$\frac{d[\text{CO}]_{pe}}{[\text{CO}]_{pe}} = 2 \frac{d[\text{OH}]}{[\text{OH}]}$$

we find

$$d \ln [\text{CO}] = \frac{1}{2\alpha} d \ln [\text{CO}]_{pe} \quad (3.43)$$

If $\alpha = 2$, a 10-fold decrease in $[\text{OH}]$ and therefore a 100-fold decrease in $[\text{CO}]_{pe}$ yield only a factor of 3 decrease in $[\text{CO}]$. Thus the CO oxidation reactions may be considered to be effectively quenched for $\alpha > 2$.

We now need to evaluate α to determine whether or not the CO partial equilibrium is maintained. The rate of decay of the hydroxyl concentration is tied to the other reaction intermediates through the fast exchange reactions 2-7. The partial equilibrium assumption greatly simplifies the analysis of an otherwise very complex kinetics problem. There are several ways to evaluate the partial equilibrium. We have identified a number of reactions (2-7) that maintain the partial equilibrium among the reaction intermediates. We now need to develop a description of how the entire pool of intermediates evolves due to reactions other than 2-7. This can be done by following a weighted sum of the

concentrations of the species in that pool, i.e.,

$$P = [\text{OH}] + a[\text{O}] + b[\text{H}_2] + c[\text{H}] + d[\text{HO}_2] + e[\text{H}_2\text{O}_2]$$

P is defined such that it is not affected by reactions 2-7. Other reactions are needed for it to change. If, for example, the temperature were changed, the distribution of reaction intermediates would change as described by (3.38); but as long as the partial equilibrium is maintained, the value P will remain unchanged unless other reactions take place. If we write

$$R_2 = k_{+2}[\text{H}][\text{O}_2] - k_{-2}[\text{OH}][\text{O}]$$

$$R_3 = k_{+3}[\text{O}][\text{H}_2] - k_{-3}[\text{OH}][\text{H}] \quad \text{etc.}$$

The time rate of change of P may be written

$$\rho \frac{d(P/\rho)}{dt} = (R_2 + R_3 - R_4 + 2R_5 - R_6) + a(R_2 - R_3 - R_5) + b(-R_3 - R_4) + c(-R_2 + R_3 + R_4) + d(-R_6 + 2R_7) + e(-R_7) + R_p$$

where R_p is the total contribution of other reactions to the time rate of change of P . Rearranging, we have

$$\rho \frac{d(P/\rho)}{dt} = R_2(1 + a - c) + R_3(1 - a - b + c) + R_4(-1 - b + c) + R_5(2 - a) + R_6(-1 - d) + R_7(2d - e) + R_p \quad (3.44)$$

At the partial equilibrium, the net contribution of reactions 2-7 to changing P must be zero regardless of the rates of the individual reactions. This condition is satisfied by setting the coefficients of each of the rates equal to zero. This yields

$$P = [\text{OH}] + 2[\text{O}] + 2[\text{H}_2] + 3[\text{H}] - [\text{HO}_2] - 2[\text{H}_2\text{O}_2] \quad (3.45)$$

Three-body recombination reactions are responsible for the decrease in P as the combustion products cool. These reactions include

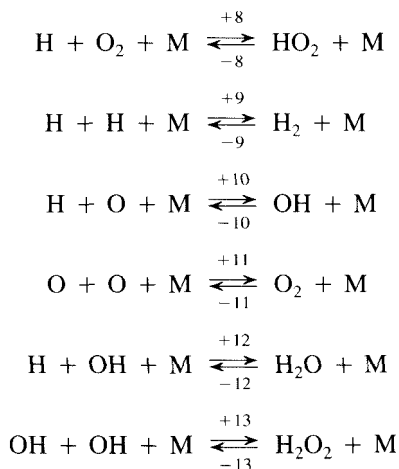


TABLE 3.4 CARBON MONOXIDE OXIDATION AND RECOMBINATION REACTION RATES

Reaction	Rate coefficient
$\text{CO} + \text{OH} \xrightarrow{+1} \text{CO}_2 + \text{H}$	$k_{+1} = 4.4 T^{1.5} \exp(+372/T) \text{ m}^3 \text{ mol}^{-1} \text{ s}^{-1}$
$\text{H} + \text{O}_2 + \text{M} \xrightarrow{+8} \text{HO}_2 + \text{M}$	$k_{+8} = 1.5 \times 10^{13} \exp(500/T) \text{ m}^6 \text{ mol}^{-2} \text{ s}^{-1}$
$\text{H} + \text{H} + \text{M} \xrightarrow{+9} \text{H}_2 + \text{M}$	$k_{+9} = 6.4 \times 10^5 T^{-1} \text{ m}^6 \text{ mol}^{-2} \text{ s}^{-1}$
$\text{H} + \text{O} + \text{M} \xrightarrow{+10} \text{OH} + \text{M}$	$k_{+10} = 1.0 \times 10^4 \text{ m}^6 \text{ mol}^{-2} \text{ s}^{-1}$
$\text{O} + \text{O} + \text{M} \xrightarrow{+11} \text{O}_2 + \text{M}$	$k_{+11} = 1.0 \times 10^5 T^{-1} \text{ m}^6 \text{ mol}^{-2} \text{ s}^{-1}$
$\text{H} + \text{OH} + \text{M} \xrightarrow{+12} \text{H}_2\text{O} + \text{M}$	$k_{+12} = 1.4 \times 10^{11} T^{-2} \text{ m}^6 \text{ mol}^{-2} \text{ s}^{-1}$
$\text{OH} + \text{OH} + \text{M} \xrightarrow{+13} \text{H}_2\text{O}_2 + \text{M}$	$k_{+13} = 1.3 \times 10^{10} T^{-2} \text{ m}^6 \text{ mol}^{-2} \text{ s}^{-1}$

The forward rate constants for these reactions are summarized in Table 3.4. In fuel-lean combustion, reaction 8 is the predominant recombination reaction at equilibrium, but other reactions may become important at nonequilibrium states.

The rate of change in P may be written

$$\begin{aligned} \rho \frac{d(P/\rho)}{dt} = & -4k_{+8}[\text{H}][\text{O}_2][\text{M}] + 4k_{-8}[\text{HO}_2][\text{M}] - 4k_{+9}[\text{H}][\text{H}][\text{M}] \\ & + 4k_{-9}[\text{H}_2][\text{M}] - 4k_{+10}[\text{H}][\text{O}][\text{M}] + 4k_{-10}[\text{OH}][\text{M}] \\ & - 4k_{+11}[\text{O}][\text{O}][\text{M}] + 4k_{-11}[\text{O}_2][\text{M}] - 4k_{+12}[\text{H}][\text{OH}][\text{M}] \\ & + 4k_{-12}[\text{H}_2\text{O}][\text{M}] - 4k_{+13}[\text{OH}][\text{OH}][\text{M}] + 4k_{-13}[\text{H}_2\text{O}_2][\text{M}] \end{aligned}$$

where the factors of 4 result from the net change of P as one mole recombines. Using the partial equilibrium concentrations of the reaction intermediates, we find

$$\begin{aligned} \rho \frac{d(P/\rho)}{dt} = & -(4k_{+8}[\text{H}][\text{O}_2][\text{M}] + 4k_{+9}[\text{H}][\text{H}][\text{M}] + 4k_{+10}[\text{H}][\text{O}][\text{M}] \\ & + 4k_{+11}[\text{O}][\text{O}][\text{M}] + k_{+12}[\text{H}][\text{OH}][\text{M}] \\ & + 4k_{+13}[\text{OH}][\text{OH}][\text{M}]) \left(1 - \frac{[\text{OH}]_e^4}{[\text{OH}]^4} \right) \end{aligned} \quad (3.46)$$

where the subscript e denotes the concentration at full thermodynamic equilibrium.

P may be expressed in terms of any of the reaction intermediates. In terms of hydroxyl, (3.46) becomes

$$\begin{aligned}
 \rho \frac{d[\text{OH}]/\rho}{dt} = & - \left[\frac{4k_{+8}[\text{OH}]_e^3[\text{M}]}{K_2 K_5 [\text{H}_2\text{O}]} y^3 + \frac{4k_{+9}[\text{OH}]_e^6[\text{M}]}{K_2^2 K_5^2 [\text{H}_2\text{O}]^2 [\text{O}_2]} y^6 \right. \\
 & + \frac{4k_{+10}[\text{OH}]_e^5[\text{M}]}{K_2 K_5^2 [\text{O}_2] [\text{H}_2\text{O}]^2} y^5 + \frac{4k_{+11}[\text{OH}]_e^4[\text{M}]}{K_5^2 [\text{H}_2\text{O}]^2} y^4 \\
 & \left. + \frac{4k_{+12}[\text{OH}]_e^4[\text{M}]}{K_2 K_5 [\text{H}_2\text{O}] [\text{O}_2]} y^4 + 4k_{+13}[\text{OH}]_e^2[\text{M}] y^2 \right] \left(1 - \frac{1}{y^4} \right) \\
 & \div [1 + Ay + By^2 + Cy^{-2} + Dy^{-3}]
 \end{aligned} \tag{3.47}$$

where

$$y = \frac{[\text{OH}]}{[\text{OH}]_e}$$

and

$$A = 4 \left(\frac{[\text{O}]_e}{[\text{OH}]_e} + \frac{[\text{H}_2]_e}{[\text{OH}]_e} \right)$$

$$B = 9 \frac{[\text{H}]_e}{[\text{OH}]_e}$$

$$C = \frac{[\text{HO}_2]_e}{[\text{OH}]_e}$$

$$D = \frac{4[\text{H}_2\text{O}_2]_e}{[\text{OH}]_e}$$

In terms of y , P becomes

$$\begin{aligned}
 P = & [\text{OH}]_e y + 2[\text{O}]_e y^2 + 2[\text{H}_2]_e y^2 \\
 & + 3[\text{H}]_e y^3 - [\text{HO}_2]_e y^{-1} - [\text{H}_2\text{O}_2]_e y^{-2}
 \end{aligned} \tag{3.48}$$

The coefficients depend on fuel composition (C/H ratio), temperature, and equivalence ratio. Only for extreme deviations from equilibrium or for near stoichiometric or fuel-rich combustion will the reaction intermediates be present in high enough concentrations to alter the concentrations of the major species appreciably and thus to modify the coefficients. Limiting our attention to fuel-lean combustion, (3.47) can now be used to evaluate α and to determine the conditions for which the CO partial equilibrium can be maintained:

$$\alpha = \frac{E_8 y + E_9 y^4 + E_{10} y^3 + E_{11} y^2 + E_{12} y^2 + E_{13}}{1 + Ay + By^2 + Cy^{-2} + Dy^{-3}} (1 - y^{-4}) \tag{3.49}$$

where

$$E_8 = \frac{4k_{+8}[\text{OH}]_e[\text{M}]}{k_{+1}K_2K_5[\text{H}_2\text{O}]}$$

$$E_9 = \frac{4k_9[\text{OH}]_e^4[\text{M}]}{k_{+1}K_2^2K_5^2[\text{H}_2\text{O}]^2[\text{O}_2]^2}$$

$$E_{10} = \frac{4k_{+10}[\text{OH}]_e^3[\text{M}]}{k_{+1}K_2K_5^2[\text{H}_2\text{O}]^2[\text{O}_2]}$$

$$E_{11} = \frac{4k_{+11}[\text{OH}]_e^2[\text{M}]}{k_{+1}K_5^2[\text{H}_2\text{O}]^2}$$

$$E_{12} = \frac{4k_{+12}[\text{OH}]_e^2[\text{M}]}{k_{+1}K_2K_5[\text{H}_2\text{O}][\text{O}_2]}$$

$$E_{13} = \frac{4k_{+13}[\text{M}]}{k_{+1}}$$

Figure 3.13 shows the variation of α with y for combustion of aviation kerosene in air at an equivalence ratio of 0.91 and atmospheric pressure. To examine the quenching of CO oxidation, we limit our attention to the decrease of P from an initial value

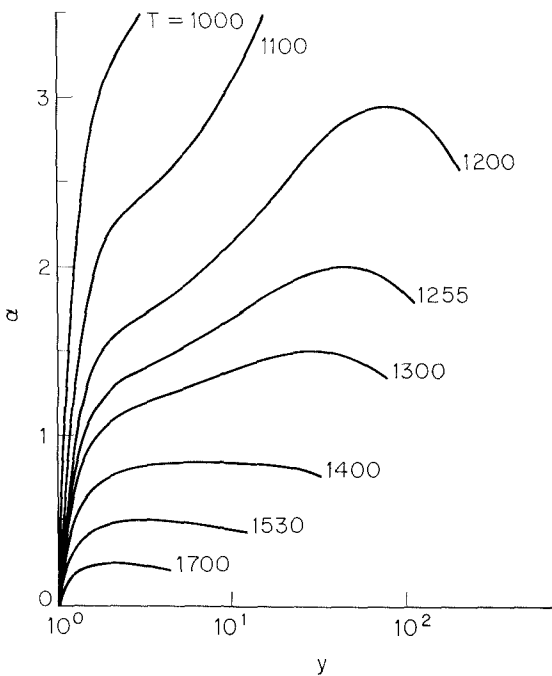


Figure 3.13 Variation of α with y for various temperatures. The maximum value of y for each temperature corresponds to the value at which P equals the value at 2000 K.

corresponding to thermodynamic equilibrium in the flame region. Values of y falling in the shaded region correspond to P greater than that at 2000 K and therefore are not of interest here. At temperatures above 1530 K, α is less than $\frac{1}{2}$ for all y , so the carbon monoxide partial equilibrium will be maintained regardless of cooling rate. Since

$$[\text{CO}]_{pe} = [\text{CO}]_e y^2 \tag{3.50}$$

the CO levels can still be much larger than the equilibrium value. The very rapid initial rise of α with y means that it is very difficult to maintain the partial equilibrium at low temperatures. At 1000 K, y must be smaller than 1.04 for the partial equilibrium to hold.

Complete quenching of CO oxidation requires α to be larger than about 2. This occurs only at temperatures below 1255 K. At 1000 K, α is less than 2 for $y < 1.25$. If cooling is sufficiently rapid such that the recombination reactions are unable to maintain the radical concentrations very close to equilibrium, CO will begin to deviate from the partial equilibrium below 1450 K and will be fully frozen between 1000 and 1100 K. The level at which the CO concentration will freeze depends strongly on the deviation from equilibrium of the concentration of reaction intermediates.

The cooling rate for which y equals a specified value can be used to estimate the maximum cooling rate that will lead to acceptable CO emissions. Our analysis of Figure 3.13 has provided guidelines on the values of y for which CO will be oxidized or frozen. To eliminate the temperature dependence of the concentrations in our calculations, it is convenient to express y in terms of mole fractions, that is,

$$y = \frac{x_{\text{OH}}}{x_{\text{OH},e}}$$

noting that this formulation also requires that the total number of moles in the combustion products (or the mean molecular weight) not change significantly due to the recombination reactions. This limits the analysis to fuel-lean combustion products.

y is a function of time through x_{OH} and of temperature through $x_{\text{OH},e}$. The time rate of change of y is thus

$$\frac{dy}{dt} = \frac{1}{x_{\text{OH},e}} \frac{dx_{\text{OH}}}{dt} - \frac{x_{\text{OH}}}{x_{\text{OH},e}^2} \frac{dx_{\text{OH},e}}{dT} \frac{dT}{dt}$$

To cool at constant y , $dy/dt = 0$, so

$$\frac{dT}{dt} = \frac{(1/x_{\text{OH}})(dx_{\text{OH}}/dt)}{d \ln x_{\text{OH},e}/dT} \tag{3.51}$$

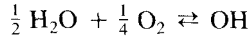
Substituting (3.42) yields

$$\frac{dT}{dt} = -\frac{\alpha k_1 c x_{\text{OH},e} y^2}{d \ln x_{\text{OH},e}/dT} \tag{3.52}$$

where c is the molar concentration of the gas.

The equilibrium OH concentration can be expressed in terms of species whose

concentrations will not vary significantly with T by the reaction



that is,

$$x_{\text{OH},e} = K_{p,\text{OH}} x_{\text{H}_2\text{O}}^{1/2} x_{\text{O}_2}^{1/4} p^{-1/4}$$

Thus

$$\frac{d \ln x_{\text{OH},e}}{dT} = \frac{d \ln K_{p,\text{OH}}}{dT}$$

Van't Hoff's equation, (2.41), can be used to develop expressions for the equilibrium constants:

$$\begin{aligned} K_{p2} &= 13.2e^{-8220/T} & K_{p4} &= 0.241e^{7670/T} \\ K_{p5} &= 9.64e^{-8690/T} & K_{p6} &= 0.0822e^{36,600/T} \\ K_{p,\text{OH}} &= 159e^{-19,620/T} & K_{p7} &= 6.50e^{-21,155/T} \end{aligned}$$

Using these equilibrium constants and the rate coefficients from Table 3.4, the cooling rate for which y will remain constant may be evaluated. Cooling rates corresponding to several values of y are shown in Figure 3.14. For any value of y , the allowable cooling rate decreases rapidly as T decreases. The limits of maintenance of the CO partial equilibrium ($\alpha = 0.5$) and freezing of CO oxidation ($\alpha = 2$) for constant y cooling are also shown. It is clear that very slow cooling rates are required to maintain the partial equilibrium below 1500 K. Considering that combustion products are generally cooled by 1000 to 2000 K before being exhausted, this slow cooling can be achieved only in systems with residence times in excess of 1 s. Thus the CO partial equilibrium might be maintained to 1500 K in utility boilers, but not in many smaller systems and certainly not in engines where the total residence time may be tens of milliseconds or less. As we have noted previously, complete quenching of the CO oxidation only occurs below 1255 K. At high cooling rates, deviations from the CO partial equilibrium begin at the limiting temperature of 1450 K. As the cooling rate is increased, the value of y and, therefore, the CO partial equilibrium level also increase.

Prediction of the actual CO emission levels from a combustion system requires integration of the chemical rate equations through the cooling process. The CO equilibrium is rapidly established in the high-temperature region of most flames, so equilibrium provides a reasonable initial condition for the examination of oxidation quenching in flames.

We can now see the reasons for the variation in the global rate expressions of Table 3.3. Rates 1 and 2 corresponded to carbon monoxide oxidation in an equilibrated pool of reaction intermediates. This corresponds to

$$R_{\text{CO}} = -k_1[\text{OH}]_e \{ [\text{CO}] - [\text{CO}]_{pe} \}$$

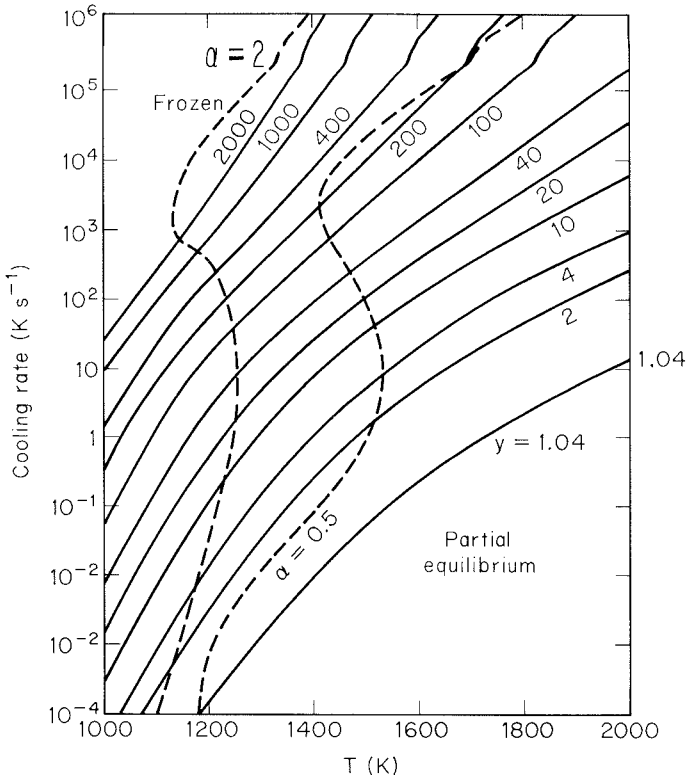


Figure 3.14 Cooling rates corresponding to constant values of y as a function of temperature. The cooling rates corresponding to the onset of deviations from partial equilibrium ($\alpha = 0.5$) and complete quenching of CO oxidation ($\alpha = 2$) are indicated by the dashed curves. The region of partial quenching is shaded.

Rate 3 was determined within the flame where radicals are present in superequilibrium concentrations.

$$R_{CO} = -k_1 [OH]_e y \{ [CO] - [CO]_{pe} \}$$

The excess of radicals over equilibrium (value for y) for which this rate expression was derived is specific to the flame in which the rate was measured. It might correspond to a particular nonflame situation, but different cooling rates will clearly lead to different radical concentrations. Thus no one global expression is universally applicable. In contrast to the global models, the partial-equilibrium approach provides an estimate of the radical concentration corresponding to a particular cooling history.

To apply the partial-equilibrium model, rate equations for both the pool of reaction intermediates and carbon monoxide must be integrated. Again expressing the concentra-

tion of intermediate species in terms of OH, the equations become

$$R_{\text{OH}} = -k_1[\text{OH}]_e^2 \alpha y^2$$

$$R_{\text{CO}} = -k_1[\text{OH}]_e y \{ [\text{CO}] - [\text{CO}]_e y^2 \}$$

where α is given by (3.49).

As a test of this model, we shall compare theoretical predictions with the data of Morr and Heywood (1974), who examined carbon monoxide oxidation quenching in a plug-flow, kerosene-fired laboratory combustor. After combustion products were fully mixed ($S < 0.05$) and equilibrated, they were passed through a heat exchanger which, at $\phi = 0.91$, dropped the temperature from 2216 K to 975 K in about 5 ms (i.e., a cooling rate of about $2 \times 10^5 \text{ K s}^{-1}$). The equilibrium CO concentration decreases rapidly upon cooling, but the measured concentrations decrease much more slowly, as illustrated in Figure 3.15.

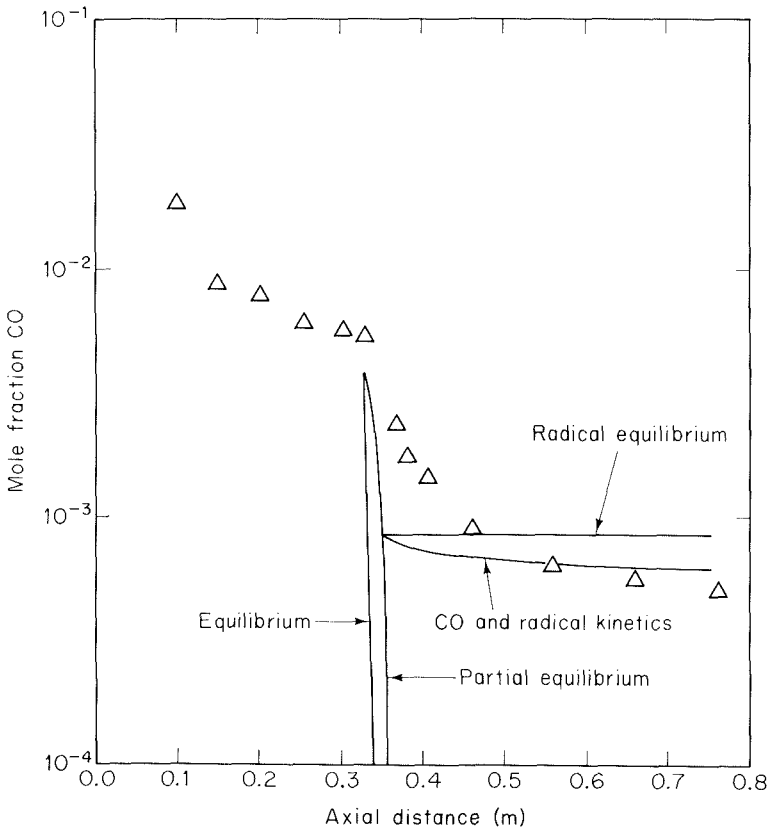


Figure 3.15 Comparison of measured and calculated carbon monoxide profiles as a function of axial position in a plug flow combustor with a heat exchange (data from Morr and Heywood, 1974).

Three predictions of the CO level, obtained by numerical integration of the rate equations, are also shown in Figure 3.15. If CO is assumed to be equilibrated with OH, its concentration decreases rapidly to levels far below the measurements. The prediction for equilibrium OH shows a rapid initial rate of CO oxidation, with the reactions being completely frozen within the heat exchanger due to the very low equilibrium OH concentration at low temperature. This contrasts markedly with the slower but continuous decrease in CO that was observed. The partial equilibrium model, including both the recombination reactions and CO oxidation, yields a slightly more gradual decline in the CO level. The ultimate predictions are in close agreement with the experimental data. Thus we see that both the recombination reactions and the carbon monoxide oxidation reactions are important to CO oxidation.

The treatment presented here is subject to a number of limiting assumptions, notably (1) the members of the radical pool must all be minor species so that the concentrations of H_2O and O_2 are constant, and (2) the mean molecular weight must be constant. Detailed modeling of CO formation and destruction in flames or in stoichiometric or fuel-rich combustion products requires that these constraints be eliminated. Calculation of the partial equilibrium by direct minimization of the Gibbs free energy as described by Keck and Gillespie (1971) and Morr and Heywood (1974) allows the model developed here to be applied in general without such restrictions. Furthermore, the Gibbs free-energy minimization code can be applied without the tedious algebra since chemical reaction constraints can be treated in exactly the same way as element conservation constraints to the minimization problem.

3.3 HYDROCARBONS

Like CO, hydrocarbon emissions from combustion systems result from incomplete combustion. Equilibrium levels of hydrocarbons are low at the equivalence ratios at which practical combustion systems are normally operated, and the oxidation reactions are fast. Hydrocarbons can escape destruction if poor mixing allows very fuel-rich gases to persist to the combustor exhaust or if the oxidation reactions are quenched early in the combustion process.

The composition and quantity of hydrocarbons in exhaust gases depend on the nature of the fuel and of the process that limits oxidation. The range of hydrocarbon species that are emitted from combustion systems is too broad to present a detailed accounting here. Polycyclic aromatic hydrocarbons (PAH) are a particularly significant class of combustion-generated hydrocarbons since they include a number of known carcinogens or mutagens. These compounds form in extremely fuel-rich regions of the flame, where hydrocarbon polymerization reactions are favored over oxidation. Figure 3.16 illustrates pathways that are thought to lead to a number of PAH species. The complexities and uncertainties in hydrocarbon oxidation mechanisms make a detailed analysis beyond the scope of this book. Rough estimates of hydrocarbon emission rates can be made using global oxidation models such as those discussed in Chapter 2, but quantitative models have yet to be developed. Combustion conditions that result in low

Basis: Add C₂, C₃, or C₄ to form 5- or 6-membered rings (no 5-5 adjacent)
(no more than 2 5-membered rings)

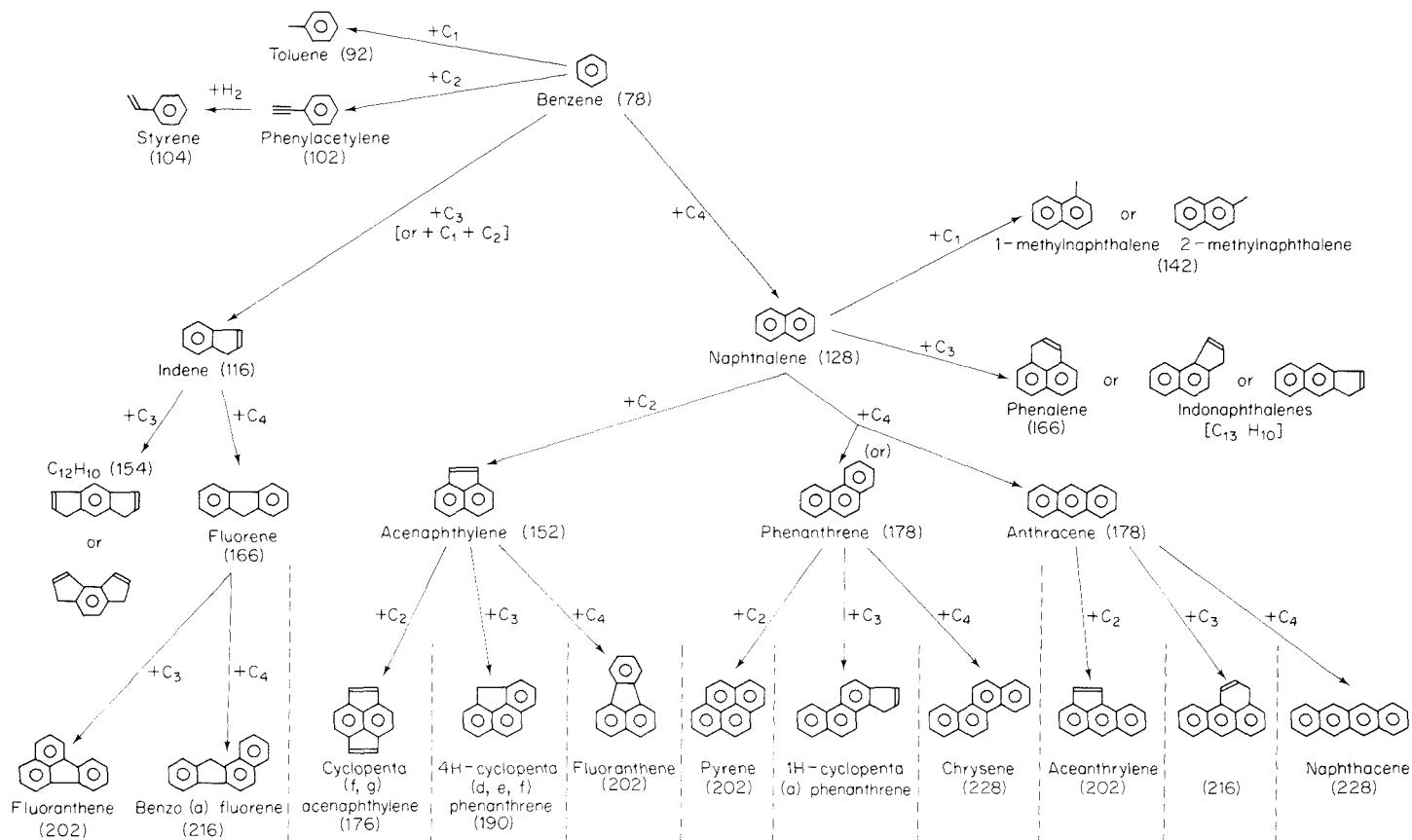
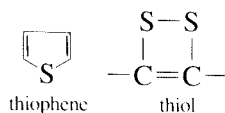


Figure 3.16 Mechanisms of polycyclic aromatic hydrocarbon formation and growth (courtesy of A. Sarofim). The numbers in parenthesis are the molecular weights.

carbon monoxide emission will generally yield low exhaust concentrations of unburned hydrocarbons. Noncombustion sources of hydrocarbons, such as fuel or lubricant evaporation, are frequently major contributors to hydrocarbon emissions.

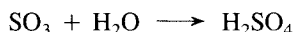
3.4 SULFUR OXIDES

Coal and heavy fuel oils contain appreciable amounts of sulfur (Tables 2.2 and 2.3). The dominant inorganic sulfur species in coal is pyrite (FeS_2). Organic sulfur forms include thiophene, sulfides, and thiols (Attar, 1978):



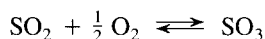
In fuel-lean combustion, the vast majority of this sulfur is oxidized to form SO_2 . Sulfides, predominantly H_2S and COS , may survive in fuel-rich flames (Kramlich et al., 1981). All of these compounds are considered air pollutants. The sulfides are odoriferous as well. Sulfur removal, either from the fuel or from the combustion products, is required for emission control.

A fraction of the sulfur is further oxidized beyond SO_2 to form SO_3 (Barrett et al., 1966). Sulfur trioxide is a serious concern to boiler operators since it corrodes combustion equipment. When combustion products containing SO_3 are cooled, the SO_3 may react with water to form sulfuric acid,



which condenses rapidly at ambient temperatures to form a fine sulfuric acid aerosol that frequently appears as a blue fume near the stack outlet.

The equilibrium level of SO_3 in fuel-lean combustion products is determined by the overall reaction

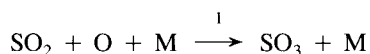


Applying van't Hoff's equation to the data of Table 2.5, we find

$$K_p = 1.53 \times 10^{-5} e^{11,760/T} \text{ atm}^{-1/2}$$

We see that the equilibrium yield of SO_3 increases with decreasing temperature. In combustion products below about 900 K, SO_3 would be the dominant species at chemical equilibrium. Actual conversion of SO_2 to SO_3 is too slow to reach the equilibrium level.

SO_3 is formed primarily by the reaction



for which Westenberg and de Haas (1975) recommended a rate coefficient of

$$k_1 = 8.0 \times 10^4 e^{-1400/T} \text{ m}^6 \text{ mol}^{-2} \text{ s}^{-1}$$

SO₃ can also react with O,



where the rate constant is

$$k_2 = 7.04 \times 10^4 e^{785/T} \quad \text{m}^6 \text{mol}^{-2} \text{s}^{-1}$$

Another possible sink for SO₃ is



Muller et al. (1979) have estimated

$$k_3 = 1.5 \times 10^7 \text{ m}^3 \text{mol}^{-1} \text{s}^{-1}$$

The destruction of SO₃ is dominated by these radical reactions rather than by the thermal decomposition of SO₃ (Fenimore and Jones, 1965; Cullis and Mulcahy, 1972). At the low temperatures where SO₃ is formed, the endothermic reverse reactions are not important, so the rate equation for SO₃ may be written

$$R_{\text{SO}_3} = k_1[\text{SO}_2][\text{O}][\text{M}] - k_2[\text{SO}_3][\text{O}][\text{M}] - k_3[\text{SO}_3][\text{H}]$$

If we assume constant-temperature, fuel-lean combustion, this becomes

$$\frac{d[\text{SO}_3]}{dt} = k_1[\text{O}][\text{M}]\{[S_T] - [\text{SO}_3]\} - \{k_2[\text{O}][\text{M}] + k_3[\text{H}]\}[\text{SO}_3]$$

where [S_T] is the total concentration of sulfur oxides. Further assuming that the concentrations of the radicals are constant, this may be integrated to determine [SO₃]:

$$[\text{SO}_3] = \frac{k_1[S_T][\text{O}][\text{M}]}{k_1[\text{O}][\text{M}] + k_2[\text{O}][\text{M}] + k_3[\text{H}]} (1 - e^{-t/\tau}) + [\text{SO}_3]_0 e^{-t/\tau}$$

where

$$\tau = \{k_1[\text{O}][\text{M}] + k_2[\text{O}][\text{M}] + k_3[\text{H}]\}^{-1}$$

and [SO₃]₀ denotes the amount of SO₃ formed in the flame where the H and O concentrations are not equilibrated. At large time, SO₃ approaches a steady-state level

$$[\text{SO}_3]_{ss} = \frac{k_1[S_T][\text{O}][\text{M}]}{k_1[\text{O}][\text{M}] + k_2[\text{O}][\text{M}] + k_3[\text{H}]}$$

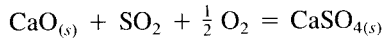
Assuming equilibrium O and H, the characteristic time for SO₃ oxidation is about 0.009 s for $\phi = 0.9$ at 1700 K, but increases to 0.13 s at 1500 K. Thus the reactions become quite slow as the combustion products are cooled below 1500 K, where the equilibrium yield becomes appreciable.

Steady-state SO₃ levels are on the order of 10% of the total sulfur in fuel-lean combustion products at low temperatures. Actual conversions are frequently lower, on the order of 3%. Clearly, the steady state is not maintained throughout the cooling pro-

cess. The quenching of SO_2 oxidation is directly coupled to the radical chemistry that was discussed in conjunction with CO oxidation. Rapid cooling leads to superequilibrium radical concentrations and the maintenance of the SO_3 steady state at lower temperatures than the foregoing estimates of chemical relaxation times would suggest.

Sulfur dioxide oxidation is catalyzed by metals such as vanadium, so SO_3 production in some systems is much greater than the homogeneous gas-phase chemistry would suggest. SO_3 yields as high as 30% have been reported for combustion of some high-vanadium fuel oils. These high levels produce an acidic aerosol that has been called "acid smut." In extreme cases, plumes become opaque due to the condensation of water on the hygroscopic acid aerosol. Fuel additives such as MgO have been used to control such SO_3 formation.

Sulfur reactions with inorganic species can be used, under special circumstances, to retain sulfur in the solid phase so that it can be removed from combustion products with particulate emission control equipment. We consider processes in Chapter 8 that use such species for gas cleaning. A commonly used sorbent is lime, CaO, which reacts with sulfur oxides to form calcium sulfate, or gypsum,



The equilibrium constant for this SO_2 capture reaction is

$$K_p = 1.17 \times 10^{-14} e^{58,840/T} \text{ atm}^{-3/2}$$

The equilibrium mole fraction of SO_2 is

$$y_{\text{SO}_2} = p^{-3/2} K_p^{-1} y_{\text{O}_2}^{-1/2}$$

Thus low temperatures and fuel-lean combustion favor the retention of SO_2 as calcium sulfate. For combustion products containing 3% oxygen ($\phi = 0.85$) the equilibrium SO_2 level is below 100 ppm for temperatures below about 1360 K. Sulfur capture in the combustion zone is most promising for systems in which the peak temperatures are low [e.g., fluidized-bed or fixed-bed (stoker-fired) combustors]. The high temperatures typical of pulverized coal flames promote the decomposition of any CaSO_4 that may be formed to CaO and SO_2 . While sulfur capture is favored thermodynamically as the products of pulverized coal combustion cool, the reactivity of lime that is processed through high-temperature flames is reduced dramatically by sintering or fusion that reduces the surface area on which the sulfur capture reactions can take place.

A major application of sorbents for in-flame sulfur capture is in fluidized-bed combustors where the temperature must be kept low to prevent ash agglomeration. In fluidized-bed combustors, relatively large (millimeter-sized) coal particles are fluidized by an airflow from below at a velocity that lifts the particles but does not entrain them and carry them out of the bed. To keep the temperature below the ash fusion temperature, the coal bed is diluted with a large excess of noncombustible particles. If limestone or another sorbent is used as the diluent, the release of fuel sulfur from the flame can be effectively minimized.

The reactions leading to sulfur capture take place on the surface of the CaO. The active surface includes large numbers of small pores that are generated as the lime is

produced by calcination of limestone, CaCO_3 . The density of CaCO_3 is 2710 kg m^{-3} , considerably smaller than that of CaO , 3320 kg m^{-3} , but the mass loss in calcination at temperatures below about 1400 K occurs without appreciable change in the dimensions of the particle (Borgwardt and Harvey, 1972). The resulting pore volume ($\approx 3.6 \times 10^{-4} \text{ m}^3 \text{ kg}^{-1}$) accounts for more than one-half of the total lime volume. The spongy material thus provides a large surface area (0.6 to $4 \text{ m}^2 \text{ g}^{-1}$) on which the surface reactions of SO_2 can take place.

Reaction of CaO to form CaSO_4 increases the solid volume by a factor of 3.3. If the particle does not expand upon reaction, the amount of CaSO_4 formed in the pores is determined by the pore volume, that is,

$$\text{volume of CaSO}_4 \text{ formed} = \text{volume of CaO reacted} + \text{pore volume}$$

This corresponds to conversion of about one-half of the CaO to CaSO_4 . Before the pore volume is filled, the reaction rate is limited by the rate of the surface reaction. For large particles, the diffusional resistance in the pores reduces the sulfur capture rate. After the pore volume is filled, SO_2 must diffuse through the solid reaction products for further reaction to take place, so the reaction rate slows considerably.

The rate of sulfur capture may be expressed in the form

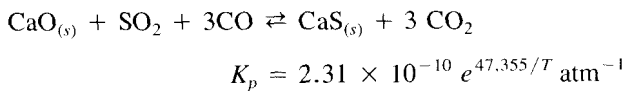
$$r_0 = k_s S_g [\text{SO}_2] \eta \quad \text{mol SO}_2 (\text{kg CaO s})^{-1}$$

where S_g is the initial surface area as measured by N_2 adsorption (BET method), and η is an effectiveness factor that accounts for the resistance to diffusion in the pore structure of the sorbent. Borgwardt and Harvey (1972) measured an intrinsic rate coefficient, k_s , of

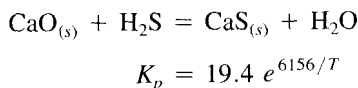
$$k_s = 135 e^{-6290/T} \quad \text{m s}^{-1}$$

For small particles, large pores, or both, the effectiveness factor may be taken as unity, and this rate may be applied directly. For larger particles, a pore transport model is required to estimate η and sulfur capture. (See Section 2.8.2.)

Within fixed beds, in the early fuel-rich regions of pulverized coal flames, and within the porous structure of burning char, the reducing atmosphere makes sulfur capture as mineral sulfides possible. For equivalence ratios not too far from unity, SO_2 may react with CaO :



In extremely fuel-rich gases, H_2S and COS are the predominant sulfur species, so reactions such as



also contribute to sulfur retention. The sulfur capture reactions are not strongly dependent on temperature at high equivalence ratios, so sulfur capture can be achieved at

higher temperatures than would be possible in a fuel-lean environment. Freund and Lyon (1982) have reported sulfur retention as high as 80% in the ash of coal that was enriched with Ca by ion exchange prior to combustion at equivalence ratios greater than 3.

Control of NO_x formation from fuel-bound nitrogen also requires combustion under fuel-rich conditions, so there has been considerable interest in combining NO_x control with in-flame sulfur capture. One version of this technology involves limestone injection in multistage (low NO_x) burners (LIMB). The limestone is calcined early in the flame and then may react with the sulfur released from the fuel. One problem is that the addition of sufficient air to complete the combustion process provides the thermodynamic driving force for the release of any sulfur that has been captured. Sintering of the sorbent at the high temperatures in the near stoichiometric regions of the flame, however, may inhibit the release of previously captured sulfur.

PROBLEMS

- 3.1. A furnace is fired with natural gas (assume methane). The inlet air and fuel temperatures are 290 K and the pressure is atmospheric. The residence time in the combustor is 0.1 s. Assuming the combustion to be adiabatic, calculate the NO mole fraction at the combustor outlet for combustion at $\phi = 0.85$.
- 3.2. Combustion products at 600 K are to be mixed with the incoming air to lower the NO emissions from the furnace in Problem 3.1. Assuming that the total mass flow rate through the furnace does not change, determine what fraction of the flue gases must be recycled to reduce NO_x formation by 90%. What is the corresponding change in the amount of heat that can be transferred to a process requiring a temperature of 600 K?
- 3.3. For the furnace of Problem 3.1, determine the equivalence ratio that would achieve a 90% reduction in NO formation. What is the corresponding change in the amount of heat that can be transferred to a process requiring a temperature of 600 K?
- 3.4. Examine the influence of mixing on NO formation by determining the amount of NO formed in the furnace of Problem 3.1 if the segregation parameter is $S = 0.3$. Assume a Gaussian equivalence ratio distribution.
- 3.5. As a model of the low NO_x burner, consider a flame in which combustion initially takes place fuel-rich, at an equivalence ratio of $\phi_1 = 1.5$, and that air is then entrained into the flame region at a constant mass entrainment rate until the flame is diluted to an equivalence ratio of $\phi_2 = 0.8$. Let the time over which this dilution takes place be τ . The flame may be assumed to be adiabatic, with no further change in ϕ occurring after an equivalence ratio of 0.8 is achieved. Calculate the NO formation when a fuel with composition $\text{CH}_{1.8}\text{N}_{0.01}$ and lower heating value of 41 MJ kg^{-1} is burned in 298 K air at atmospheric pressure. Use the effective reaction rate from Figure 3.7 and T from Figure 2.6 to calculate the rate of N_2 formation. What is the effect of increasing the entrainment time from 0.1 s to 1 s?
- 3.6. In the derivation of the model for selective reduction of NO, it was assumed that the NH_2 concentration achieved a steady state. Examine the validity of that assumption.
- 3.7. The temperature is not constant in the reaction zone where the NH_3 -NO reactions take place in practical implementations of the thermal de- NO_x process. Numerically integrate the rate

equations for the kinetic model for this system to determine the impact of cooling at a rate of 500 K s^{-1} on the temperature window of operation. Compare your results with isothermal operation. Assume that the fuel has composition CH_2 and was burned at an equivalence ratio of 0.85 and that the initial NO concentration was 400 ppm, and consider NH_3/NO ratios of 0.5, 1, and 2.

3.8. Combustion products with composition

$$y_{\text{O}_2} = 0.02$$

$$y_{\text{H}_2\text{O}} = 0.10$$

$$y_{\text{CO}_2} = 0.11$$

$$y_{\text{N}_2} = 0.77$$

$$y_{\text{NO}} = 500 \text{ ppm}$$

are cooled from 2300 K to 500 K.

- (a) Determine the equilibrium NO mole fraction as a function of temperature for this cooling process.
 - (b) Numerically integrate the NO rate equation to calculate the amount of NO formed when the cooling takes place at constant cooling rates of 1000 and 10^5 K s^{-1} .
 - (c) Determine the influence of radical nonequilibrium on NO formation by adapting the model developed to describe CO oxidation.
- 3.9. Use the rate constants presented in Table 2.7 to examine the validity of the partial-equilibrium assumption for the species H, OH, O, H_2 , HO_2 , and H_2O_2 . For combustion of $\text{CH}_{1.88}$ in atmospheric pressure air at $\phi = 0.91$ and a cooling rate of 10^4 K s^{-1} , beginning with equilibrium at 2000 K, at what temperature does the partial-equilibrium model begin to break down?

REFERENCES

- ALLEN, J. D. "Probe Sampling of Oxides of Nitrogen from Flames," *Combust. Flame*, 24, 133–136 (1975).
- ATTAR, A. "Chemistry, Thermodynamics, and Kinetics of Sulfur in Coal Gas Reactions—A Review," *Fuel*, 57, 201–212 (1978).
- AZUHATA, S., KAJI, R., AKIMOTO, H., and HISHINUMA, Y. "A Study of the Kinetics of the NH_3 -NO-O₂-H₂O₂ Reaction," in *Eighteenth Symposium (International) on Combustion*, The Combustion Institute, Pittsburgh, PA, 845–852 (1981).
- BARRETT, R. E., HUMMELL, J. D., and REID, W. T. "Formation of SO_3 in a Noncatalytic Combustor," *J. Eng. Power Trans. ASME*, A88, 165–172 (1966).
- BAULCH, D. L., DRYSDALE, D. D., HORNE, D. G., and LLOYD, A. C. *Evaluated Kinetic Data for High Temperature Reactions*, Vol. 2, *Homogeneous Gas Phase Reactions of the H₂-N₂-O₂ System*, Butterworth, London (1973).
- BORGWARDT, R. H., and HARVEY, R. D. "Properties of Carbonate Rocks Related to SO_2 Reactivity," *Environ. Sci. Technol.*, 6, 350–360 (1972).

- BOWMAN, C. T. "Kinetics of Pollutant Formation and Destruction in Combustion," *Prog. Energy Combust. Sci.*, *1*, 33-45 (1975).
- BRANCH, M. C., KEE, R. J., and MILLER, J. A. "A Theoretical Investigation of Mixing Effects in the Selective Reduction of Nitric Oxide by Ammonia," *Combust. Sci. Technol.*, *29*, 147-165 (1982).
- CERNANSKY, N. P., and SAWYER, R. F. "NO and NO₂ Formation in a Turbulent Hydrocarbon/Air Diffusion Flame," in *Fifteenth Symposium (International) on Combustion*, The Combustion Institute, Pittsburgh, PA, 1039-1050 (1975).
- CULLIS, C. F., and MULCAHY, M. F. R. "The Kinetics of Combustion of Gaseous Sulfur Compounds," *Combust. Flame*, *18*, 225-292 (1972).
- DEAN, A. M., HARDY, J. E., and LYON, R. K. "Kinetics and Mechanism of NH₃ Oxidation," in *Nineteenth Symposium (International) on Combustion*, The Combustion Institute, Pittsburgh, PA, 97-105 (1982).
- DIEHL, L. A. "Reduction of Aircraft Gas Turbine Pollutant Emissions—A Status Report," 71st Annual Meeting, Air Pollution Control Assoc., 78-26.4 (1979).
- DRYER, F. L. and GLASSMAN, I. "High Temperature Oxidation of Carbon Monoxide and Methane," in *Fourteenth Symposium (International) on Combustion*, The Combustion Institute, Pittsburgh, PA, 987-1003 (1974).
- FENIMORE, C. P., and JONES, G. W. "Sulfur in the Burnt Gas of Hydrogen-Oxygen Flames," *J. Phys. Chem.*, *69*, 3593-3597 (1965).
- FENIMORE, C. P., and MOORE, J. "Quenched Carbon Monoxide in Fuel-Lean Flame Gases," *Combust. Flame*, *22*, 343-351 (1974).
- FLAGAN, R. C., and APPLETON, J. P. "A Stochastic Model of Turbulent Mixing with a Chemical Reaction: Nitric Oxide Formation in a Plug-Flow Burner," *Combust. Flame*, *23*, 249-267 (1974).
- FLAGAN, R. C., GALANT, S., and APPLETON, J. P. "Rate Constrained Partial Equilibrium Models for the Formation of Nitric Oxide from Organic Fuel Nitrogen," *Combust. Flame*, *22*, 299-311 (1974).
- FREUND, H., and LYON, R. K. "The Sulfur Retention of Calcium-Containing Coal during Fuel-Rich Combustion," *Combust. Flame*, *45*, 191-203 (1982).
- FRISTROM, R. M. and WESTENBERG, A. A. *Flame Structure*, McGraw-Hill, New York (1965).
- HANSON, R. K., and SALIMIAN, S. "Survey of Rate Constants in the N-H-O System," in *Combustion Chemistry*, W. C. Gardiner, Ed., Springer-Verlag, New York, 361-421 (1984).
- HARGREAVES, K. J. A., HARVEY, R., ROPER, F., and SMITH, D. B. "Formation of NO₂ in Laminar Flames," in *Eighteenth Symposium (International) on Combustion*, The Combustion Institute, Pittsburgh, PA, 133-142 (1981).
- HAYNES, B. S., IVERACH, D., and KIROV, N. Y. "The Behavior of Nitrogen Species in Fuel Rich Hydrocarbon Flames," in *Fifteenth Symposium (International) on Combustion*, The Combustion Institute, Pittsburgh, PA, 1103-1112 (1975).
- HAZARD, H. R. "Conversion of Fuel Nitrogen to NO_x in a Compact Combustor," *J. Eng. Power Trans. ASME*, *A96*, 185-188 (1974).
- HOWARD, J. B., WILLIAMS, G. C., and FINE, D. H. "Kinetics of Carbon Monoxide Oxidation in Postflame Gases," in *Fourteenth Symposium (International) on Combustion*, The Combustion Institute, Pittsburgh, PA, 975-986 (1973).

- KECK, J. C., and GILLESPIE, D. "Rate-Controlled Partial-Equilibrium Method for Treating Reacting Gas Mixtures," *Combust. Flame*, 17, 237-241 (1971).
- KRAMLICH, J. C., MALTE, P. C., and GROSSHANDLER, W. L. "The Reaction of Fuel Sulfur in Hydrocarbon Combustion," in *Eighteenth Symposium (International) on Combustion*, The Combustion Institute, Pittsburgh, PA, 151-161 (1981).
- LAVOIE, G. A., HEYWOOD, J. B., and KECK, J. C. "Experimental and Theoretical Study of Nitric Oxide Formation in Internal Combustion Engines," *Combust. Sci. Technol.*, 3, 313-326 (1970).
- LEVY, A. "Unresolved Problems in SO_x , NO_x , Soot Control in Combustion," in *Nineteenth Symposium (International) on Combustion*, The Combustion Institute, Pittsburgh, PA, 1223-1242 (1982).
- LEVY, J. M., CHAN, L. K., SAROFIM, A. F., and BEER, J. M. "NO/Char Reactions at Pulverized Coal Flame Conditions," in *Eighteenth Symposium (International) on Combustion*, The Combustion Institute, Pittsburgh, PA, 111-120 (1981).
- LUCAS, D., and BROWN, N. "Characterization of the Selective Reduction of NO by NH_3 ," *Combust. Flame*, 47, 219-234 (1982).
- LYON, R. K. "The NH_3 - NO - O_2 Reaction," *Int. J. Chem. Kinet.*, 8, 315-318 (1976).
- MILLER, J. A., BRANCH, M. C., and KEE, R. J., "A Chemical Kinetic Model for the Selective Reduction of Nitric Oxide by Ammonia," *Combust. Flame*, 43, 81-98 (1981).
- MILLER, J. A., and FISK, G. A. "Combustion Chemistry," *Chem. & Eng. News*, 22-46, August 31, 1987.
- MORR, A. R., and HEYWOOD, J. B. "Partial Equilibrium Model for Predicting Concentration of CO in Combustion," *Acta Astronautica*, 1, 949-966 (1974).
- MULLER, C. H., SCHOFIELD, K., STEINBERG, M., and BROIDA, H. P. "Sulfur Chemistry in Flames," in *Seventeenth Symposium (International) on Combustion*, The Combustion Institute, Pittsburgh, PA, 867-879 (1979).
- MUZIO, L. J., and ARAND, J. K. "Homogeneous Gas Phase Decomposition of Oxides of Nitrogen," Electric Power Research Institute Report No. EPRI FP-253, Palo Alto, CA (1976).
- MUZIO, L. J., MALONEY, K. L., and ARAND, J. K. "Reactions of NH_3 with NO in Coal-Derived Combustion Products," in *Seventeenth Symposium (International) on Combustion*, The Combustion Institute, Pittsburgh, PA, 89-96 (1979).
- PERRY, R. A., and SIEBERS, D. L. "Rapid Reduction of Nitrogen Oxides in Exhaust Gas Streams," *Nature*, 324, 657-658 (1986).
- PERSHING, D. W., and WENDT, J. O. L. "Pulverized Coal Combustion: The Influence of Flame Temperature and Coal Composition on Thermal and Fuel NO_x ," in *Sixteenth Symposium (International) on Combustion*, The Combustion Institute, Pittsburgh, PA, 389-399 (1977).
- POHL, J. H., and SAROFIM, A. F. "Devolatilization and Oxidation of Coal Nitrogen," in *Sixteenth Symposium (International) on Combustion*, The Combustion Institute, Pittsburgh, PA, 491-501 (1977).
- POMPEI, F., and HEYWOOD, J. B. "The Role of Mixing in Burner Generated Carbon Monoxide and Nitric Oxide," *Combust. Flame*, 19, 407-418 (1972).
- POPE, S. B. "PDF Methods for Turbulent Reactive Flows," *Prog. Energy Comb. Sci.*, 11, 119-192 (1985).
- SALIMIAN, S., and HANSON, R. K. "A Kinetic Study of NO Removal from Combustion Gases by Injection of NH_3 -Containing Compounds," *Combust. Sci. Technol.*, 23, 225-230 (1980).

- SAROFIM, A. F., and FLAGAN, R. C. "NO_x Control for Stationary Combustion Sources," *Prog. Energy Combust. Sci.*, 2, 1-25 (1976).
- SAROFIM, A. F., and POHL, J. "Kinetics of Nitric Oxide Formation in Premixed Laminar Flames," in *Fourteenth Symposium (International) on Combustion*, The Combustion Institute, Pittsburgh, PA, 739-754 (1973).
- WENDT, J. O. L., PERSHING, D. W., LEE, J. W. and GLASS, J. W. "Pulverized Coal Combustion: Nitrogen Oxide Formation under Fuel Rich and Staged Combustion Conditions," *Seventeenth Symposium (International) on Combustion*, The Combustion Institute, Pittsburgh, PA (1979).
- WENDT, J. O. L., and SCHULZE, O. E. "On the Fate of Fuel Nitrogen during Coal Char Combustion," *A.I.Ch.E.J.*, 22, 102-110 (1976).
- WENDT, J. O. L., STERNLING, C. V., and MATOVICH, M. A. "Reduction of Sulfur Trioxide and Nitrogen Oxides by Secondary Fuel Injection," in *Fourteenth Symposium (International) on Combustion*, The Combustion Institute, Pittsburgh, PA, 897-904 (1973).
- WESTENBERG, A. A., and DE HAAS, H. "Rate of the Reaction $O + SO_2 + M \rightarrow SO_3 + M^*$," *J. Chem. Phys.*, 63, 5411-5415 (1975).
- ZELDOVICH, Y. B., SADOVNIKOV, P. Y., and FRANK-KAMENETSKII, D. A. *Oxidation of Nitrogen in Combustion*, M. Shelef, Trans., Academy of Sciences of USSR, Institute of Chemical Physics, Moscow-Leningrad (1947).